Electronic Supplementary Material (ESI) for Materials Horizons.

SUPPORTING INFORMATION

Aggregation-induced type I&II photosensitivity and photodegradability-based molecular backbone for synergistic antibacterial and cancer phototherapy via photodynamic and photothermal therapies

*Jun Liu, [*a] Hongyu Chen,[a] Yongsheng Yang,[a] Qihui Wang,[b] Shilu Zhang,[a] Bo Zhao,[a] Zhonghui Li, Guoqiang Yang[*c] and Guowei Deng[*b]*

[a] School of pharmacy and Institute of Pharmacy, North Sichuan Medical College, Sichuan, China.

[b] College of Chemistry and Life Science, Sichuan Provincial Key Laboratory for Structural Optimization and Application of Functional Molecules, Chengdu Normal University, Chengdu, 611130, China.

[c] Institute of Chemistry & University of Chinese Academy of Sciences, Chinese Academy of Sciences, Beijing 100190, China.

Experimental Procedures

1. General Information

All chemical reagents were purchased from Beijing InnoChem Science & Technology Co (Beijing, China) and used without further purification. SOSG was purchased from Thermofisher. Absorption spectra were recorded on a Hitachi UV-3010 (Hitachi, Tokyo, Japan) and fluorescence spectra were recorded on Hitachi F7100 (Hitachi, Tokyo, Japan). ^{1}H NMR and ^{13}C NMR spectra were obtained on BrukerAvance III 400 H (400 MHz) spectrometers (Bruker, Karlsruhe, Germany). The HRMS spectra were analyzed on the Q-Exactive instrument. Zetasizer 90 (Malvern, U.K.) was selected to measure the size of the nanoparticles. We used the optical power density meter (LP-3C50, Ophir, CHINA) to calibrate the output power density to 0.4 W.cm^{-2}). A thermal imaging camera (226 s, FOTRIC, CHINA) were used to record the temperature rise process. Photoacoustic imaging was performed on multimode photoacoustic imaging system for small animals (Vevo LAZR-X, Fujifilm viualsonic, Canada).

2. Synthsis of AID 1-4 (Scheme S1).

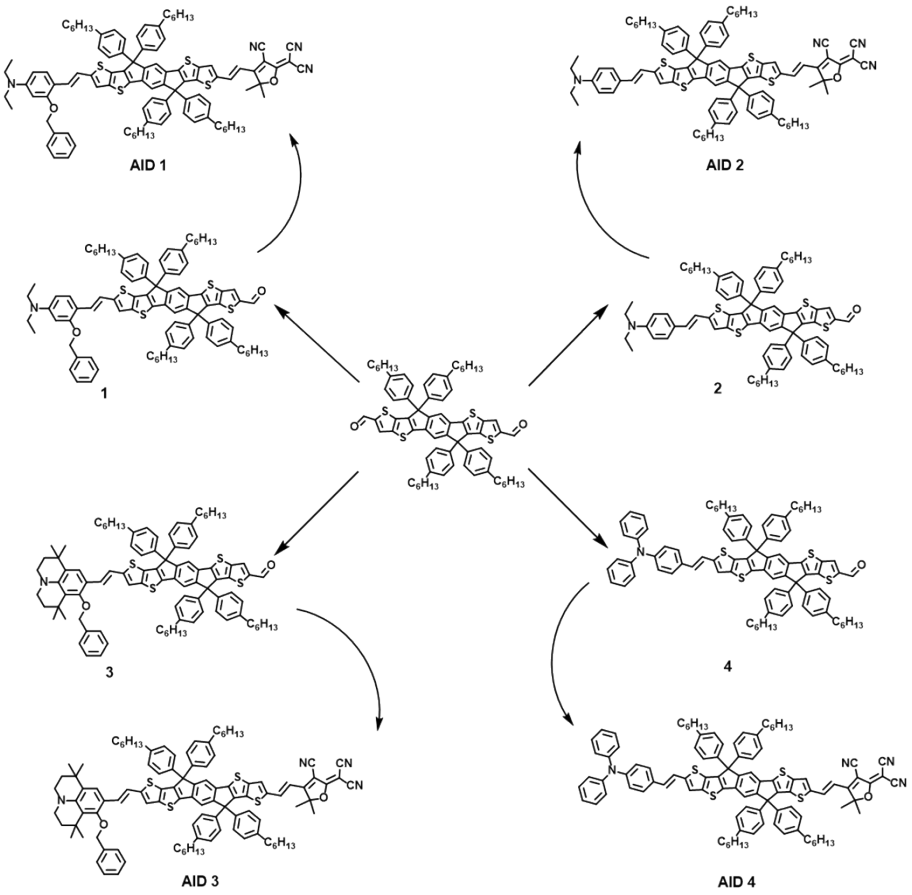

Scheme S1 the synthetic route of AID 1, AID2, AID3, and AID4.

Synthesis of C1

The benzyloxy substituted aminobenzaldehyde was reduced by NaBH4, and then reacted with triphenylphosphine hydrogen bromide to provide the phosphonate. Next, the obtained phosphonate (61mg, 0.1mmol) and IDT-2CHO (108mg, 0.1mmol) were dissolved in 5 mL 1,2-dichloroethane, and NaH (12mg, 0.5mmol) was added to the solution slowly at 0 ℃. The react mixture was stirred at room temperature for another 3 h. After poured into H_2O, the mixture was extracted by dichloromethane and dried over anhydrous Na2SO4. The solvent was removed by rotary evaporator, and the crude product was purified through column chromatography, and C1 was obtained as organic powder (yield: 60%). 1H NMR (600 MHz, CDCl3) δ 9.87 (s, 1H), 7.92 (s, 1H), 7.55 (s, 1H), 7.53 – 7.45 (m, 3H), 7.38 (t, J = 7.3 Hz, 2H), 7.33 (d, J = 6.6 Hz, 2H), 7.24 – 7.00 (m, 19H), 6.28 (d, J = 6.9 Hz, 1H), 6.17 (s, 1H), 5.15 (s, 2H), 3.29 (s,4H), 2.65 – 2.48 (m, 8H), 1.67 – 1.53 (m, 8H), 1.36 – 1.25 (m, 24H), 1.11 (s, 6H), 0.94 – 0.79 (m, 12H). 13C NMR (151 MHz, CDCl3) δ 182.77, 154.46, 153.62, 150.36, 145.61, 143.83, 142.13, 141.88, 140.47, 139.98, 139.52, 129.89, 128.73, 128.66, 128.61, 128.50, 128.19, 128.07, 127.89, 127.84, 127.17, 117.84, 104.96, 96.99, 63.04, 62.88, 44.56, 35.62, 35.58, 31.70, 31.27, 31.26, 29.20, 29.14, 22.58, 14.09. HRMS：cal for [M+] C88H95NO2S4 :1325.6246, found: 1325.6239.

Synthesis of AID1

C1(66mg, 0.05mmol), TCF (13mg, 0.065mmol) and one drop of triethylamine were dissolved in 3 mL chloroform, and the reaction was refluxed for 5h. After removed the solvent, the crude product was purified through column chromatography, and AID1 was obtained as green powder (yield: 40%). 1H NMR (400 MHz, CD2Cl2) δ 7.90 (d, J = 15.7 Hz, 1H), 7.74 (s, 1H), 7.65 (s, 1H), 7.57 (s, 1H), 7.52 (d, J = 7.1 Hz, 1H), 7.42 (t, J = 7.3 Hz, 1H), 7.37 (dd, J = 7.9, 3.7 Hz, 1H), 7.18 (tt, J = 18.6, 9.2 Hz, 1H), 6.66 (d, J = 15.7 Hz, 1H), 6.32 (dd, J = 8.8, 1.8 Hz, 1H), 6.21 (s, 1H), 5.36 (s, 1H), 3.36 (q, J = 6.9 Hz, 1H), 2.64 – 2.58 (m, 1H), 1.77 (s, 1H), 1.31 (dd, J = 15.0, 8.6 Hz, 2H), 1.15 (t, J = 7.0 Hz, 1H), 0.90 (dd, J = 7.7, 5.1 Hz, 1H). 13C NMR (101 MHz, CD2Cl2) δ 175.90, 173.02, 157.67, 154.89, 153.83, 151.21, 148.85, 147.97, 147.68, 146.08, 143.39, 143.35, 142.48, 142.21, 141.61, 141.00, 140.07, 139.78, 139.40, 139.27, 138.32, 137.61, 134.30, 130.82, 129.11, 128.74, 128.55, 128.03, 127.93, 127.78, 127.18, 124.65, 117.92, 117.71, 117.22, 116.64, 113.37, 112.23, 111.97, 111.61, 111.04, 104.95, 97.33, 96.76, 96.52, 70.51, 62.94, 62.87, 44.52, 35.50, 31.68, 31.40, 29.68, 29.14, 26.22, 22.57, 13.83, 12.41. HRMS：cal for [M+H+] C99H103N4O2S4 :1507.6958, found: 1507.6969.

Synthesis of AID2-4

Using benzyloxy substituted 1,1,7,7-tetramethyljulolidine-9-carboxaldehyde, 4-(dimethylamino)-benzaldehyde, 4-(diphenylamino) benzaldehyde as the raw materials to prepared the phosphonates repectively, the AID2-4 was synthesized according to the similar procedure as AID1.

AID2: 1H NMR (400 MHz, CD2Cl2) δ 7.90 (d, J = 15.7 Hz, 1H), 7.74 (s, 1H), 7.63 (s, 1H), 7.56 (t, J

= 3.6 Hz, 3H), 7.34 (s, 1H), 7.30 (d, J = 7.2 Hz, 1H), 7.29 (d, J = 7.7 Hz, 1H), 7.24 – 7.12 (m, 17H), 7.09 (s, 1H), 7.04 (s, 1H), 7.04 (s, 1H), 6.66 (d, J = 15.7 Hz, 1H), 4.95 (s, 2H), 3.26 – 3.21 (m, 2H), 3.17 (s, 2H), 2.61 (t, J = 7.7 Hz, 8H), 1.83-1.74 (m, 10H), 1.51 (s, 6H), 1.38 (s, 6H), 1.37-1.25 (m, 32H), 0.93 – 0.85 (m, 12H). 13C NMR (101 MHz, CD2Cl2) δ 175.78, 173.02, 155.89, 154.80, 153.83, 147.61, 146.10, 143.35, 143.25, 143.19, 142.47, 142.19, 141.01, 140.01, 139.75, 139.37, 139.26, 138.24, 137.89, 134.34, 130.98, 129.04, 128.74, 128.54, 128.43, 127.92, 127.77, 127.62, 127.33, 127.02, 125.33, 124.72, 123.90, 122.57, 122.48, 117.93, 117.57, 117.48, 116.98, 116.67, 112.20, 111.99, 111.58, 111.01, 97.30, 96.58, 76.25, 62.95, 35.50, 35.47, 32.76, 32.21, 31.67, 31.42, 31.36, 31.12, 31.02, 30.33, 29.94, 29.67, 29.15, 29.09, 26.22, 22.56, 13.81. HRMS: cal for [M+H+] C105H111N4O2S4 :1587.7584, found: 1587.7585.

AID3: 1H NMR (600 MHz, CDCl3) δ 7.77 (d, J = 15.6 Hz, 1H), 7.56 (s, 1H), 7.48 (s, 1H), 7.41 (s, 1H), 7.26 (d, J = 8.0 Hz, 2H), 7.17 (s, 1H), 7.14 – 7.01 (m, 16H), 6.93 (d, J = 15.8 Hz, 1H), 6.75 (d, J = 15.8 Hz, 1H), 6.57 (s, 2H), 6.47 (d, J = 15.6 Hz, 1H), 2.92 (s, 6H), 2.49 (m, 8H), 1.65 (s, 6H), 1.33 – 1.12 (m, 32H), 0.86 – 0.70 (m, 12H). 13C NMR (150 MHz, CDCl3) δ 175.69, 172.63, 154.87, 153.88, 151.69, 147.68, 146.12, 143.13, 143.05, 142.34, 141.99, 140.80, 140.09, 139.88, 139.82, 139.26, 138.53, 134.33, 129.11, 128.75, 128.54, 128.03, 127.84, 127.58, 117.99, 116.78, 112.19, 111.50, 111.41, 111.05, 96.92, 96.16, 62.92, 62.87, 35.59, 31.70, 31.69, 31.26, 29.70, 29.17, 26.50, 22.58, 14.09. HRMS: m/z calcd for [M+H]+ C90H93N4OS4: 1374.6258, found: 1374.6225

AID4: 1H NMR (400 MHz, CD2Cl2) δ 7.90 (d, J = 15.7 Hz, 1H), 7.74 (s, 1H), 7.66 (s, 1H), 7.62 – 7.55 (m, 1H), 7.36 (d, J = 8.7 Hz, 2H), 7.34 – 7.31 (m, 2H), 7.31 – 7.29 (m, 2H), 7.27 (s, 1H), 7.23 – 7.10 (m, 21H), 7.10 – 7.06 (m, 2H), 7.04 (d, J = 8.7 Hz, 2H), 6.88 (d, J = 16.0 Hz, 1H), 6.65 (d, J = 11.9, 1H), 2.66-2.56 (m, 8H), 1.77 (s, 6H), 1.42 – 1.25 (m, 32H), 0.92-0.84 (m, 12H). 13C NMR (101 MHz, CD2Cl2) δ 175.84, 172.98, 154.89, 153.96, 150.98, 147.64, 147.52, 147.39, 146.23, 145.81, 143.41, 143.15, 142.68, 142.50, 142.28, 141.09, 140.01, 139.67, 139.31, 139.23, 138.05, 134.64, 131.74, 130.53, 129.28, 129.12, 129.02, 128.75, 128.58, 128.09, 127.90, 127.77, 127.18, 124.69, 123.85, 123.26, 123.05, 122.48, 120.32, 118.98, 117.93, 116.86, 112.18, 112.08, 111.56, 110.99, 97.32, 96.69, 62.97, 62.92, 55.94, 35.48, 31.67, 31.37, 29.10, 26.21, 22.56, 13.81. HRMS: cal for [M+H+] C100H97N4OS4 :1497.6540, found: 1497.6515.

3. Preparation of Nanoparticles

0.1 mmol of AID1 (1.5mg), AID2 (1.59mg), AID3 (1.40mg), and AID4 (1.49mg) were respectively dissolved in 0.1 mL of acetone solution, which was poured into 1 mL of DD water under sonication (12 W). The resulted dispersion was further kept in sonication (12 W) for 5 min. The mixture was stirred in fume hood for two days.

4. Total ROS Detection by DCFH

The DMSO solution of H_2DCF-DA (2.0 mM, 20 μL) was activated by sodium hydroxide solution (0.01 M, 160 μL) and allowed to sit at room temperature for 30 min, which was added to 810 μL water and 10 uL NPs. The fluorescence signal was monitored after the solution was irradiated by 660 laser (0.4 W/cm^2) and the fluorescence spectra were recorded with the excitation wavelength at 480 nm.Control group were prepared by replacing NPs with 10uL water.

5. Detection of $^1O_2$ Generation by SOSG

$^1O_2$ generation in solution under normoxic condition were monitored with SOSG as fluorecesence probe. Briefly, 10uL SOSG in methanol (1 mM) was mixed with the AID1, AID2, AID3 and AID4 NPs water solution (working concentration: 10 μM) and irradiated by 660 nm laser (0.4 W cm^{-2}). Then, the fluorescence intensities at 530 nm for every 10s were recorded in a fluorescence spectrofluorometer (Excitation wavelength: 480nm). The $^1O_2$ generation of AID4 NPs in solution under hypoxic condition was first bubbling with N2 for 1h and then measure under N2 protection.

6. Detection of •OH Generation by APF

Aminophenyl fluorescein (APF) was used as fluorescence probe for detection of •OH in solution. 10 μM AID1, AID2, AID3, and AID4 NPs were dissolved in 1 mL water containing 10 μM of APF. The mixture was then placed in a cuvette and irradiated by 660 nm laser (0.4 W cm^{-2}). The fluorescence change of sample at 515 nm was recorded by fluorescence spectrofluorometer (Excitation wavelength: 490 nm). The •OH generation of AID4 NPs in solution under hypoxic condition was first bubbling with N2 for 1h and then measure under N_2 protection.

7. Detection of $O_2^{\bullet-}$ Generation by DHR123

Dihydrorhodamine 123 (DHR123) was used as fluorescence probe for detection of $O_2^{\bullet-}$ in solution. 10 μM AID1, AID2, AID3, and AID4 NPs were dissolved in 1 mL water containing 60 μM of DHR 123. The mixture was then placed in a cuvette and irradiated by 660 nm laser (0.4 W cm^{-2}). The fluorescence change of sample at 530 nm was recorded by fluorescence spectrofluorometer (Excitation wavelength: 480 nm). The $O_2^{\bullet-}$ generation of AID4 NPs in solution under hypoxic condition was first bubbling with N_2 for 1h and then measure under N_2 protection.

8. Cell culture, viability and imaging

4T1 cells were cultured Dul-becco's Modified Eagle Medium (DMEM) and 10% fetal bovine serum

(FBS). The cells were plated on glass bottomed dishes at 37 °C under 5% CO_2 atmosphere before experiments.

The cytotoxicity of these towards 4T1 cells was assessed by kit of CCK-8. Cells were seeded into a 96-well plate and treated with various NPs at different concentrations for 24 h. CCK-8 solution (10 μL) were added to each well, and then incubated for 2 h. The absorbance at 450 nm was recorded by microplate reader. The cell viability was deter-mined by the formula as follows. Cell viability = ($OD_{positive} - OD_{control}$)/ ($OD_{negative} - OD_{control}$). Their phototoxicity was also tested by a similar procedure, but before adding CCK8, these NPs outside the cells were washed away and exposed to white light (0.5 mW/cm^2) for 10 minutes. All the experiments were repeated three times.

4T1 cells in confocal culture dishes were preloaded with these NPs. Then, the cells were treated with H_2DCF-DA (5 μM) aqueous solution and incubated for 30 min in darkness in a 37°C cell incubator. Next, the cells were irradiated by the white light (1.5 mW/cm^2). Detection of H_2DCF-DA fluorescence was visualized by confocal microscope. H2DCF-DA was excited by a 488 nm laser, and fluorescence emission at 490-530 nm was recorded by confocal laser scanning microscopy using oil objective.

9. Photothermal properties tests in vitro

The solution of AID1, AID2, AID3 and AID4 NPs with different concentrations were irradiated by 660 nm laser (0.4 W cm $^{-2}$). The temperature changes were monitored by a IR camera.

10. Photodynamic and photothermal antibacterial effects

Suspensions of bacteria (2 μL, 10^9 estimed by McFarland Standards) in a final volume of 100 μL containing 100umol AID 1-4 NPs were in dark or irradiated 660 nm laser for 5min (0.4 W cm^{-2}), respectively. Then, the bacterial suspensions were diluted 1×10^5 fold with PBS. The diluted bacterial sample (100 μL) was spread on a solid LB agar plate, and take a picture of colonies formed after 24 h of incubation at 37 °C was counted.

11. Theoretical Calculation

All calculations were performed using the Gaussian 09 program package. The geometries of AID1, AID2, AID3 and AID4 were optimized using DFT/B3LYP/6-311G(d). The excitation energies for the singlet were predicted using TD-DFT/B3LYP/6-311G(d) based on the optimized structure in gaseous phase. The molecular orbital density is output through free software-multiwfn. [1]

12. Animals and Tumor-Bearing Mouse Model

Nude mice 6-7 weeks old were provided by the Laboratory Animal Center of North Sichuan Medical College, Nanchong, China. All procedures involving animals were performed according to a protocol approved by the Institutional Animal Care and Treatment Committee of North Sichuan Medical College. These nude mice were subcutaneously injected with 1×10^6 4T1 cells in the right anterior axillary under aseptic conditions. Then, they were individually housed under specific pathogenfree conditions with free access to food and water until the formed tumor grew to approximately 1 cm in diameter by measuring with a caliper; tumor growth to this size took about one week. These tumor-bearing mice were further used to conduct photodynamic and photothermal experiments.

13. Photodynamic and photothermal antitumor effects

The 4T1 tumor bearing mice were randomly divided into 6 groups (n = 3 for each groups), which were named "PBS + Laser", "AID1 NPs + Laser", "AID2 NPs + Laser", "AID3 NPs + Laser" and "AID4 NPs + Laser", respectively. 200 μL of PBS, "AID1 NPs (200μM)", "AID2 NPs (200μM)", "AID3 NPs (200μM)" and "AID4 NPs (200μM)", were intravenously injected into the mice, respectively. The mice were irradiated by 660 nm laser (0.4 W cm^{-2}) for 10 min post-injection, respectively. In addition, the infrared thermal images of mice were acquired by using IR camera during the irradiation of 660 nm laser (0.4W·cm^{-2}). The tumor volumes and body weight were measured every day for 8 days. Tumor volumes were measured every other day using a caliper and calculated using the following formula: volume = ((tumor length) × (tumor width) ^{2})/2. The long term survival rate was also studied by comparing the survival rate between tumor model mice receiving phototherapy in the presence of AID4 NPs and in the absence of AID4 NPs by preparing 10 mice for each group.

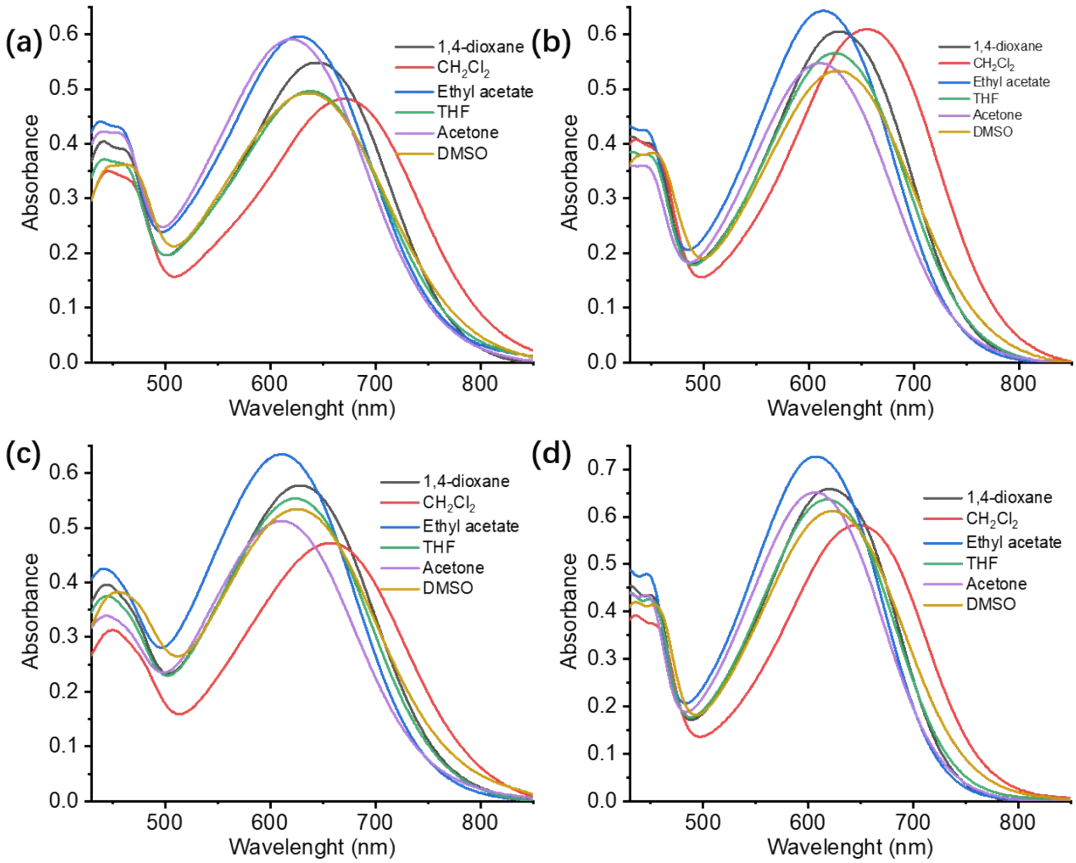

Figure S1. UV-vis absorption spectra of 10 µM (a) AID1, (d) AID2, (c) AID3 and (d) AID4 in various oganic solvents.

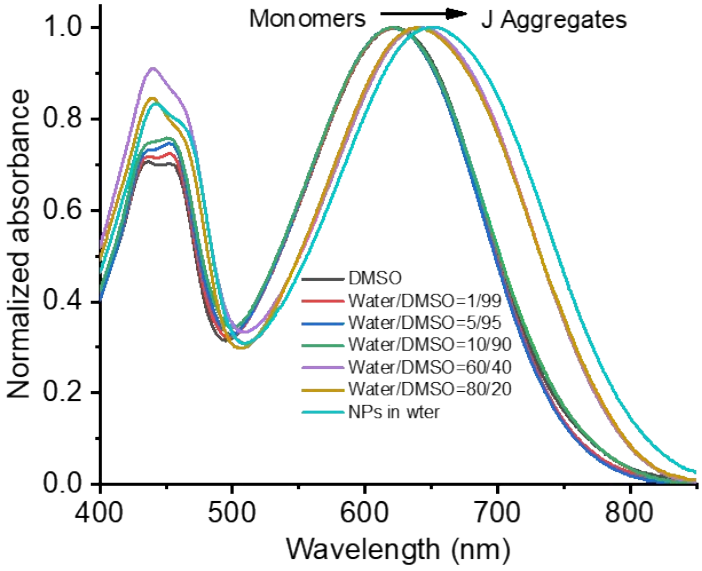

Figure S2. UV absorption of AID4 in different ratios of DMSO and water.

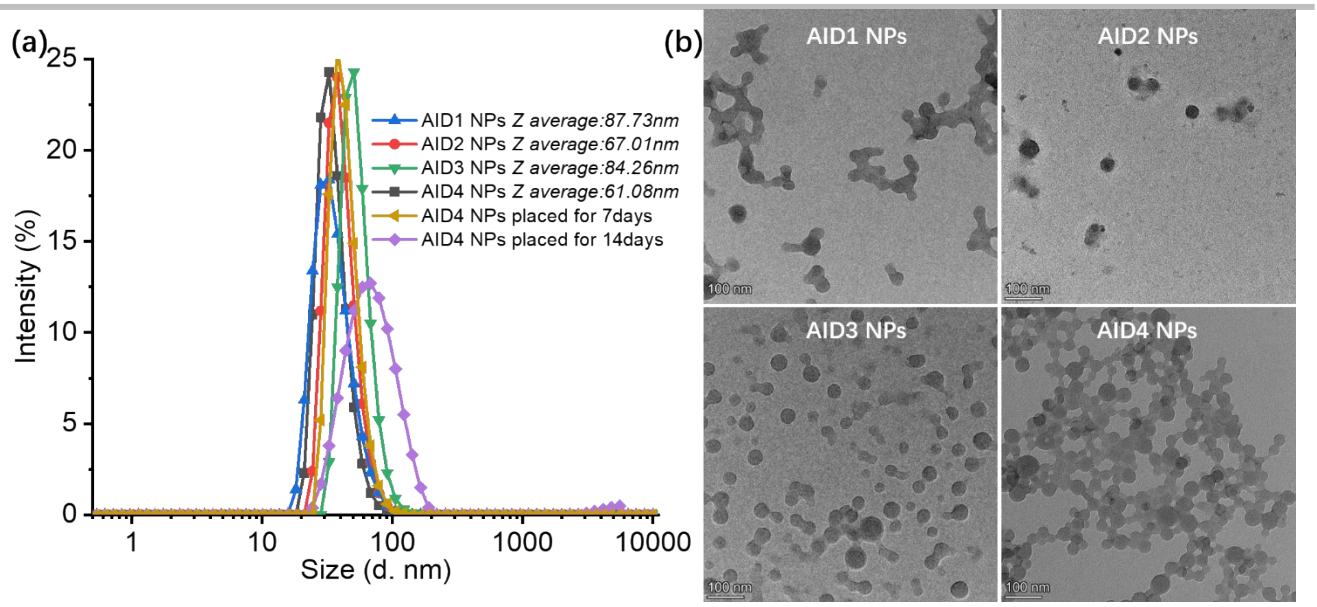

Figure S3. Size distribution of AID1 NPs, AID2 NPs, AID3 NPs and AID4 NPs measured by DLS in water . TEM image of AID1 NPs, AID2 NPs, AID3 NPs and AID4 NPs.

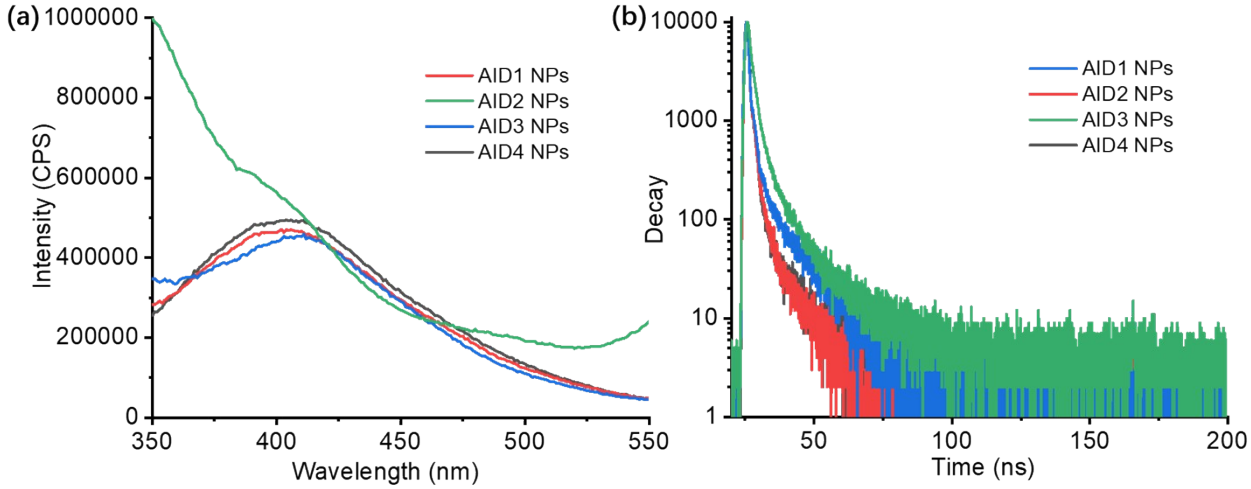

Figure S4. (a) phosphorescence spectrum and (b) phosphorescence lifetime of AID 1-4 NPs; Excitation wavelength: 350nm.

Table S1. The quantum yield of AID1 NPs, AID2 NPs, AID3 NPs and AID4 NPs.

	AID1 NPs	AID2 NPs	AID3 NPs	AID4 NPs
Quantum yield	0.04±0.02	0.03±0.02	0.04±0.02	0.05±0.02

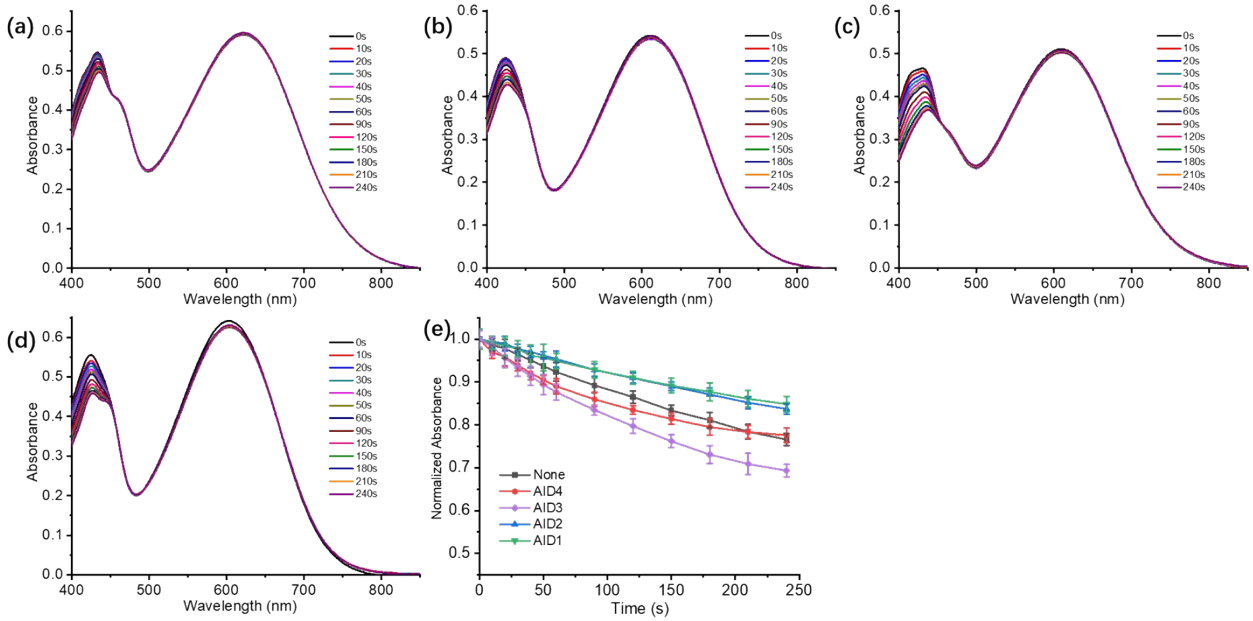

Figure S5. UV-vis absorption spectra of 10 μM (a) AID1, (b) AID2, (c)AID3 and (d) AID4 containing 10uM DPBF in acetone after 660 nm laser irradiation (0.4 W/cm^2) for different time. (e) a correlation between the absorption value at 415nm and irradiation time using 660nm laser (0.4 W/cm^2) containing 10 μM AID 1-4 and 10 uM DPBF in acetone.

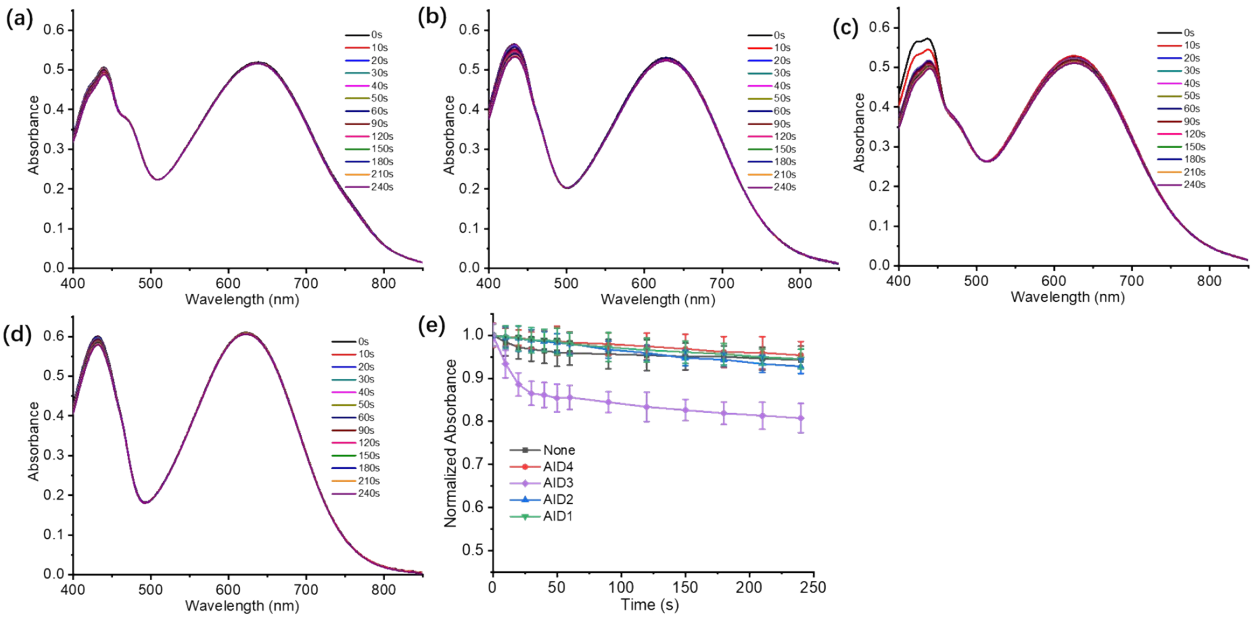

Figure S6. UV-vis absorption spectra of 10 μM (a) AID1, (b) AID2, (c)AID3 and (d) AID4 containing 10uM DPBF in DMSO after 660 nm laser irradiation (0.4 W/cm^2) for different time. (e) a correlation between the absorption value at 415nm and irradiation time using 660nm laser (0.4 W/cm^2) containing 10 μM AID 1-4 and 10 uM DPBF in DMSO.

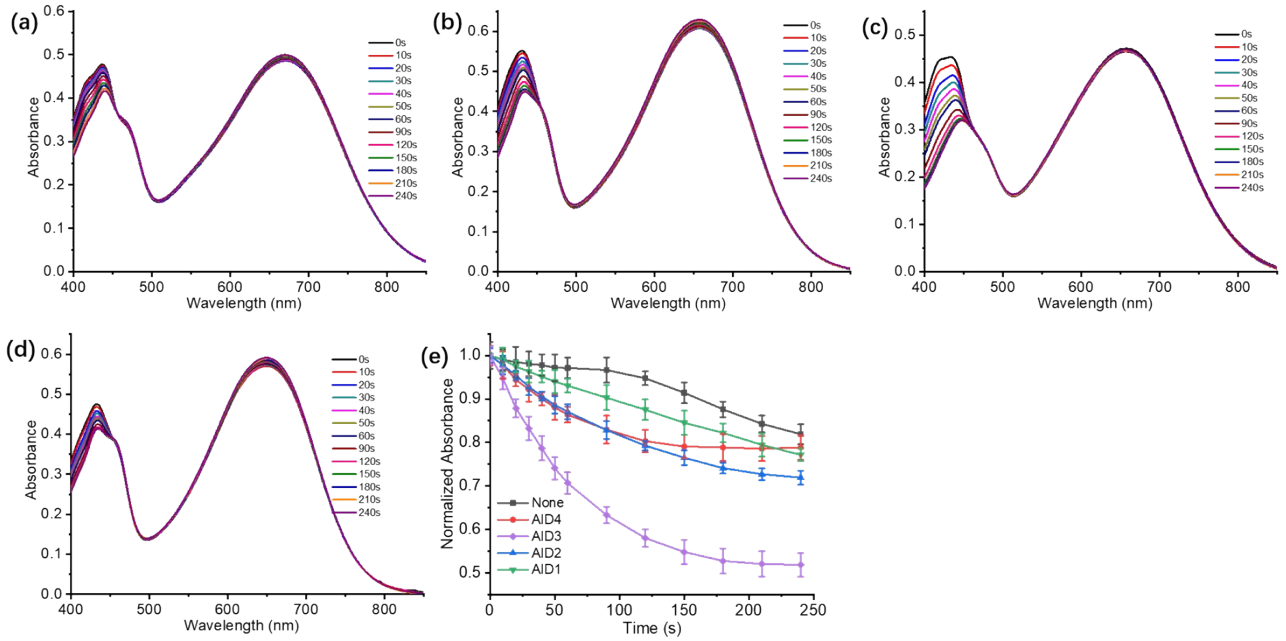

Figure S7. UV-vis absorption spectra of 10 μM (a) AID1, (b) AID2, (c)AID3 and (d) AID4 containing 10uM DPBF in CH_2Cl_2 after 660 nm laser irradiation (0.4 W/cm^2) for different time. (e) a correlation between the absorption value at 415nm and irradiation time using 660nm laser (0.4 W/cm^2) containing 10 μM AID 1-4 and 10 uM DPBF in CH_2Cl_2.

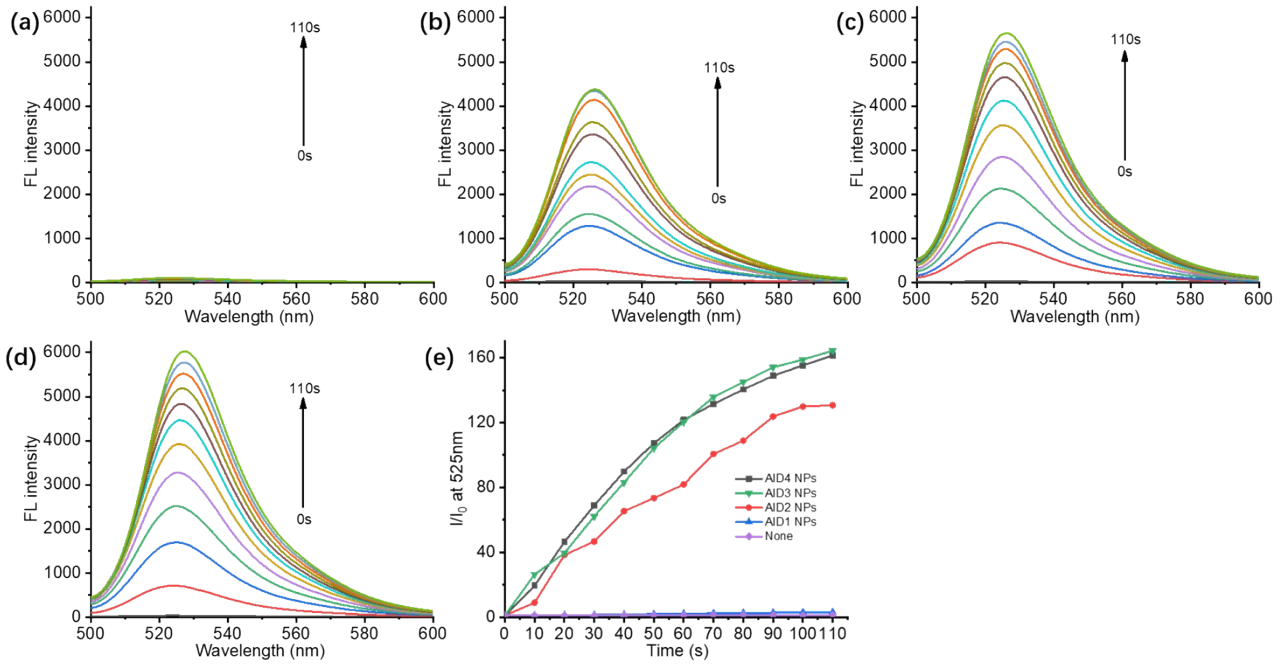

Figure S8. Fluorescence spectra changes of DCFH for total ROS detection. (a) AID1 NPs, (b) AID2 NPs, (c) AID3 NPs and (d) AID4 NPs (10 μM) with increasing irradiation time upon 660 nm laser irradiation (0.4 W cm^{-2}). (e) a correlation between the fluorescence (I/I_0) at 525nm and irradiation time using 660nm laser (0.4 W/cm^2) by using DCFH as a fluorescence probe for ROS.

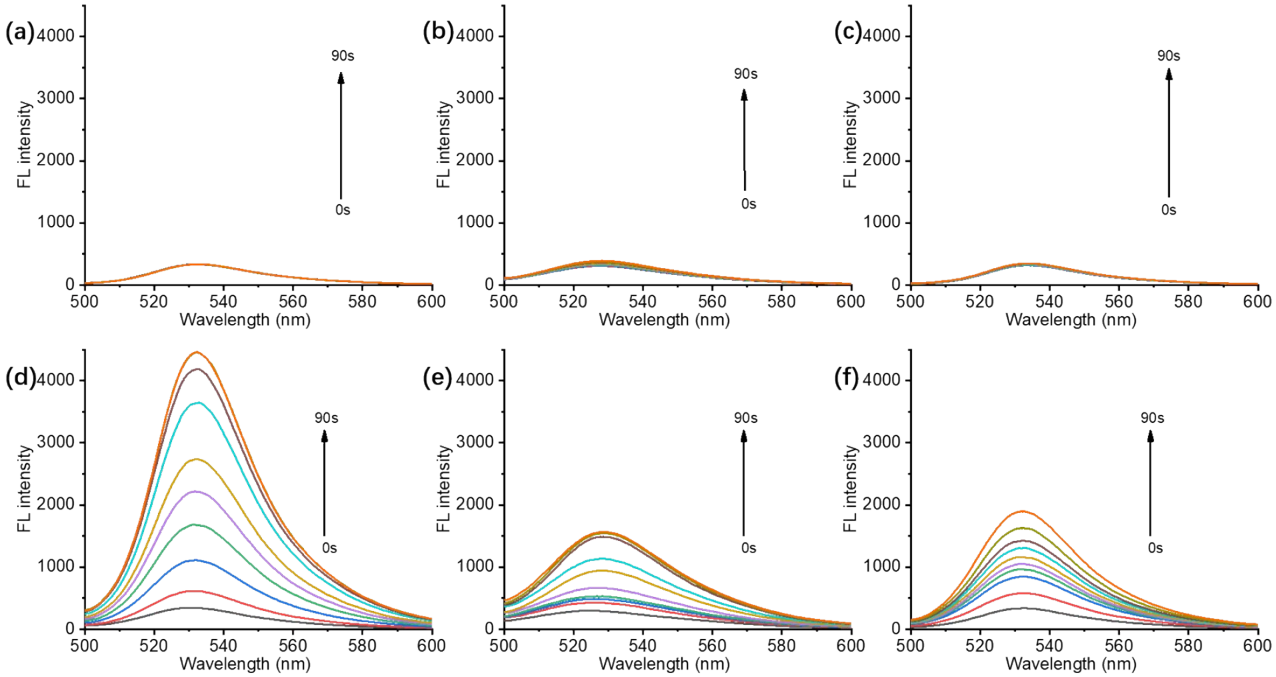

Figure S9. Fluorescence spectra changes of Singlet Oxygen Sensor Green (SOSG) for $^1O_2$ detection.. (a) AID1 NPs(10 μM), (b) AID2 NPs(10 μM), (c) AID3 NPs(10 μM) , (d) AID4 NPs (10 μM), (e) MB (10 μM) and (f) AID4 NPs(10 μM) under hypoxic environment with increasing irradiation time upon 660 nm laser irradiation (0.4 W cm^{-2}).

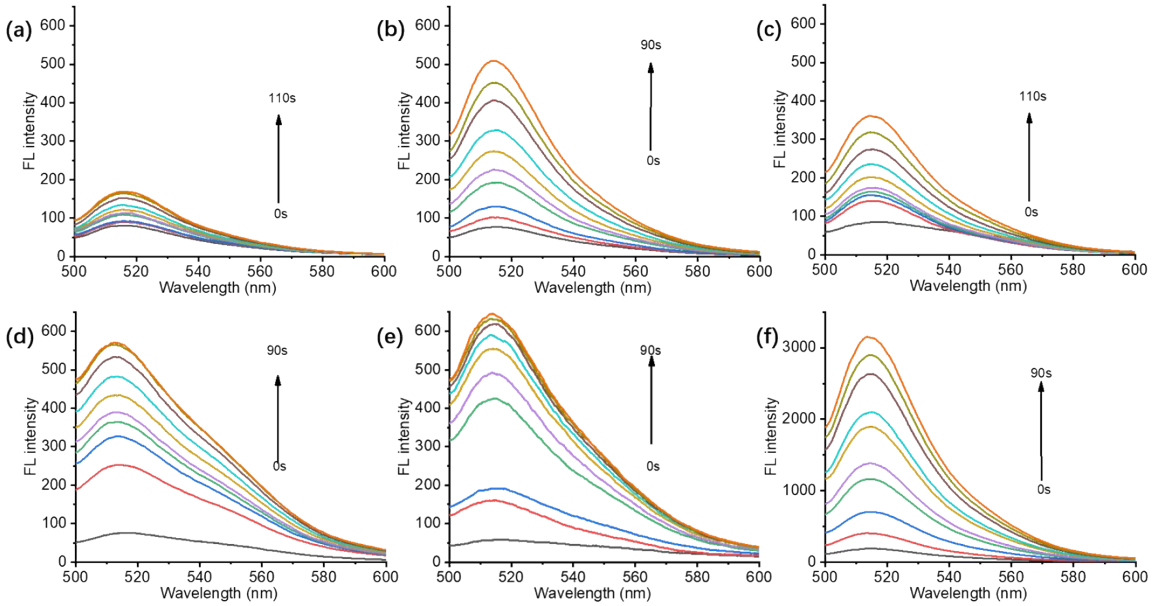

Figure S10. Fluorescence spectra changes of APF for •OH detection. (a) AID1 NPs(10 μM), (b) AID2 NPs(10 μM), (c) AID3 NPs(10 μM) , (d) AID4 NPs (10 μM), (e) MB (10 μM) and (f) AID4 NPs(10 μM) under hypoxic environment with increasing irradiation time upon 660 nm laser irradiation (0.4 W cm^{-2}).

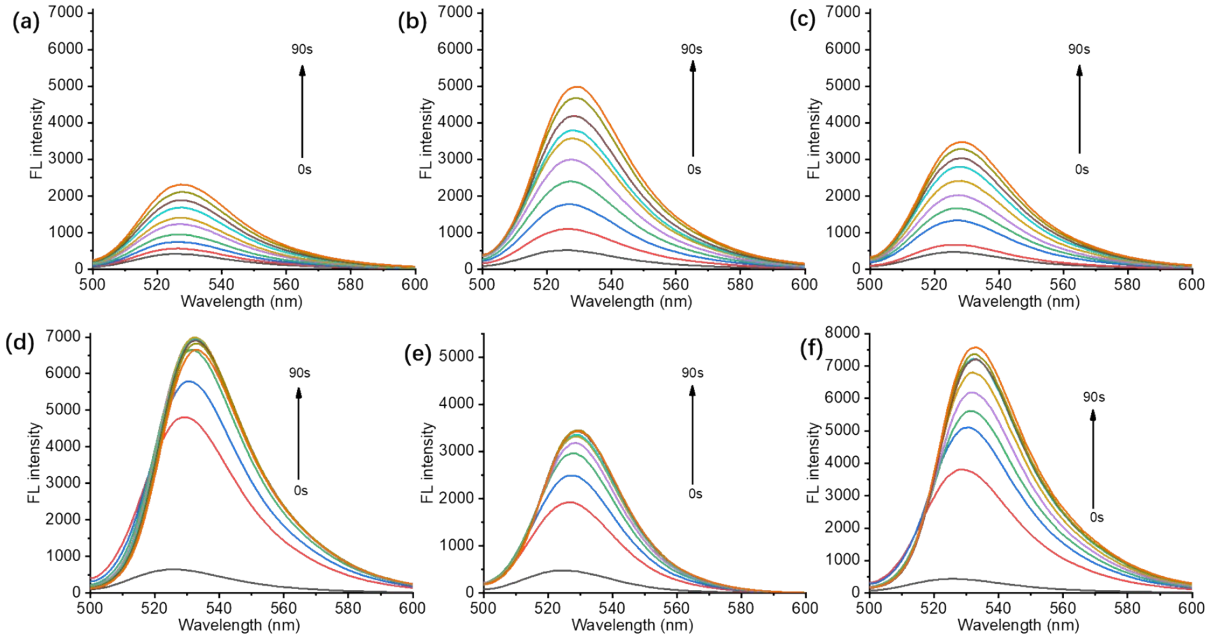

Figure S11. Fluorescence spectra changes of DHR123 for $O_2^{\bullet-}$ detection. (a) AID1 NPs(10 μM), (b) AID2 NPs(10 μM), (c) AID3 NPs(10 μM) , (d) AID4 NPs (10 μM), (e) MB (10 μM) and (f) AID4 NPs(10 μM) under hypoxic environment with increasing irradiation time upon 660 nm laser irradiation (0.4 W cm^{-2}).

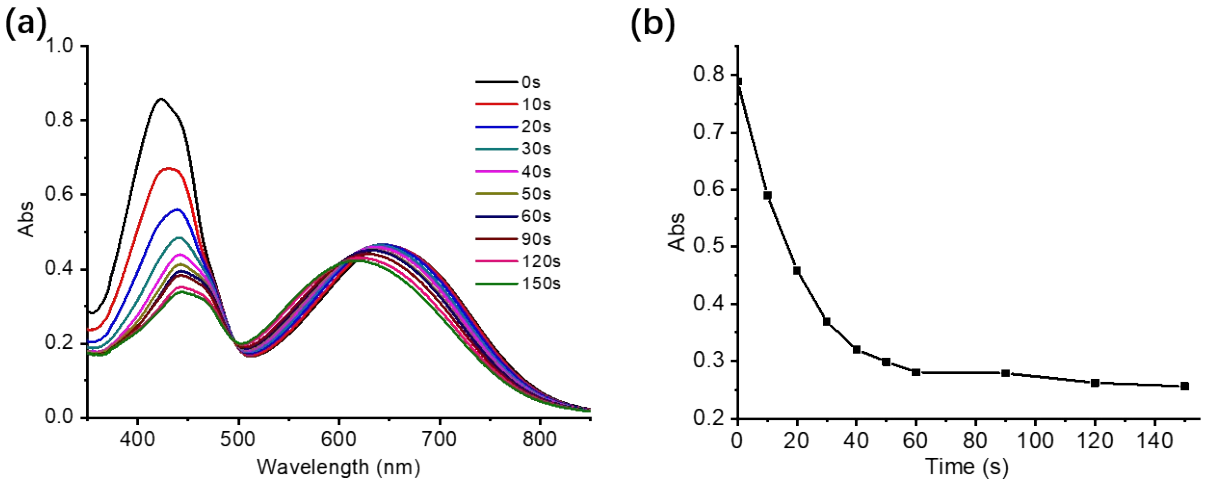

Figure S12. (a) UV-vis absorption spectra of 10 μM AID4 NPs containing 10uM DPBF in water after 660 nm laser irradiation (0.4 W/cm^2) for different time. (b) a correlation between the absorption value at 415nm and irradiation time.

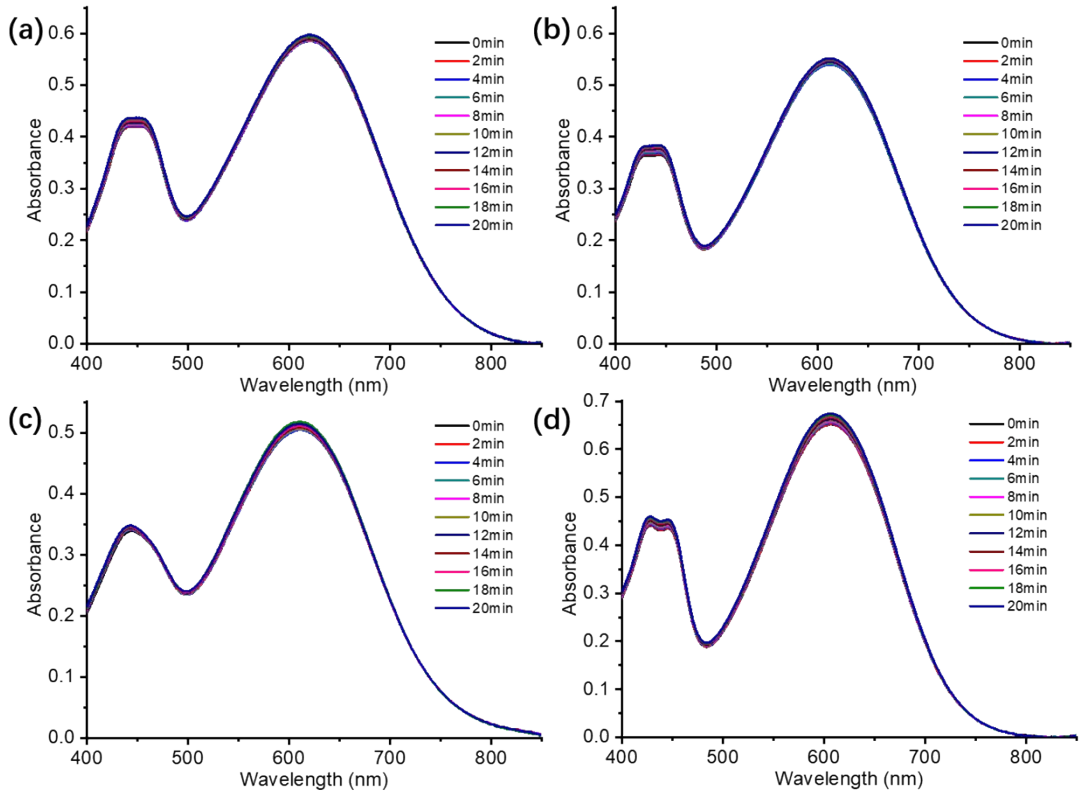

Figure S13. UV-vis absorption spectra of 10 μM (a) AID1, (d) AID2, (c) AID3 and (d) AID4 in acetone after 660 nm laser irradiation (0.4 W/cm^2) with different time.

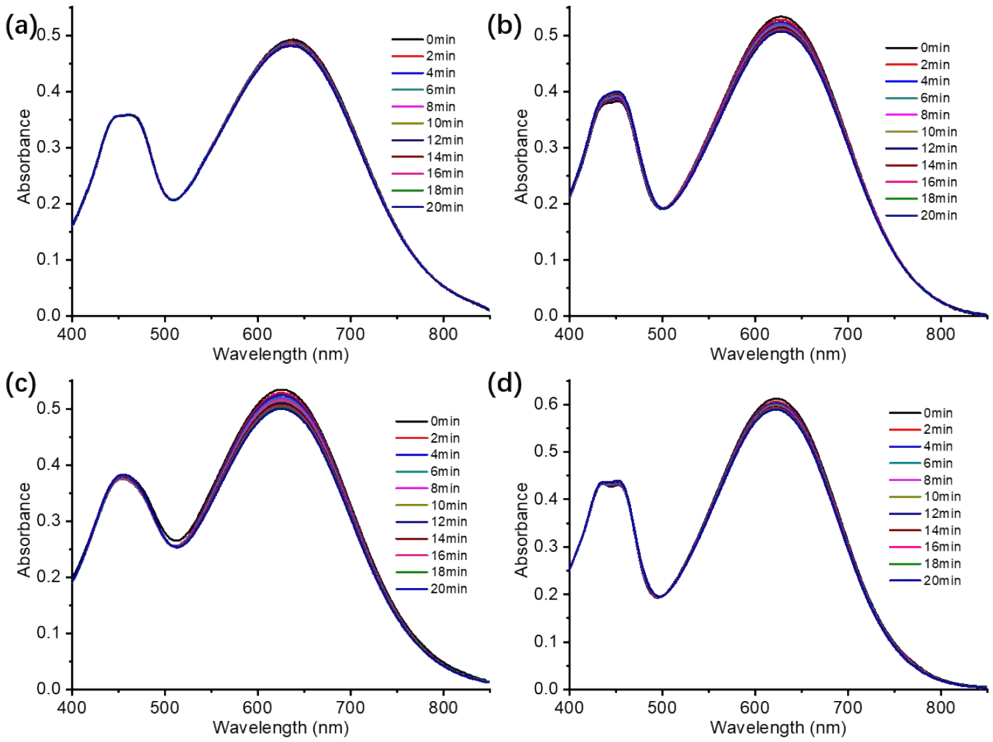

Figure S14. UV-vis absorption spectra of 10 μM (a) AID1, (d) AID2, (c) AID3 and (d) AID4 in DMSO after 660 nm laser irradiation (0.4 W/cm^2) with different time.

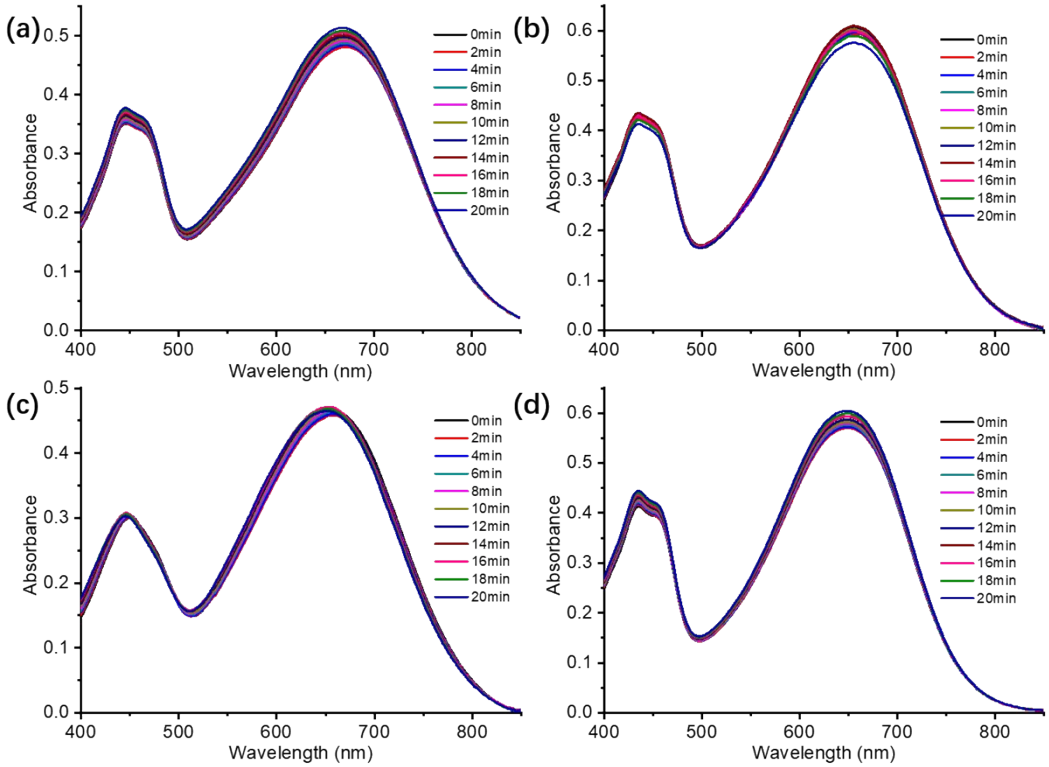

Figure S15. UV-vis absorption spectra of 10 μM (a) AID1, (d) AID2, (c) AID3 and (d) AID4 in CH_2Cl_2 after 660 nm laser irradiation (0.4 W/cm^2) with different time.

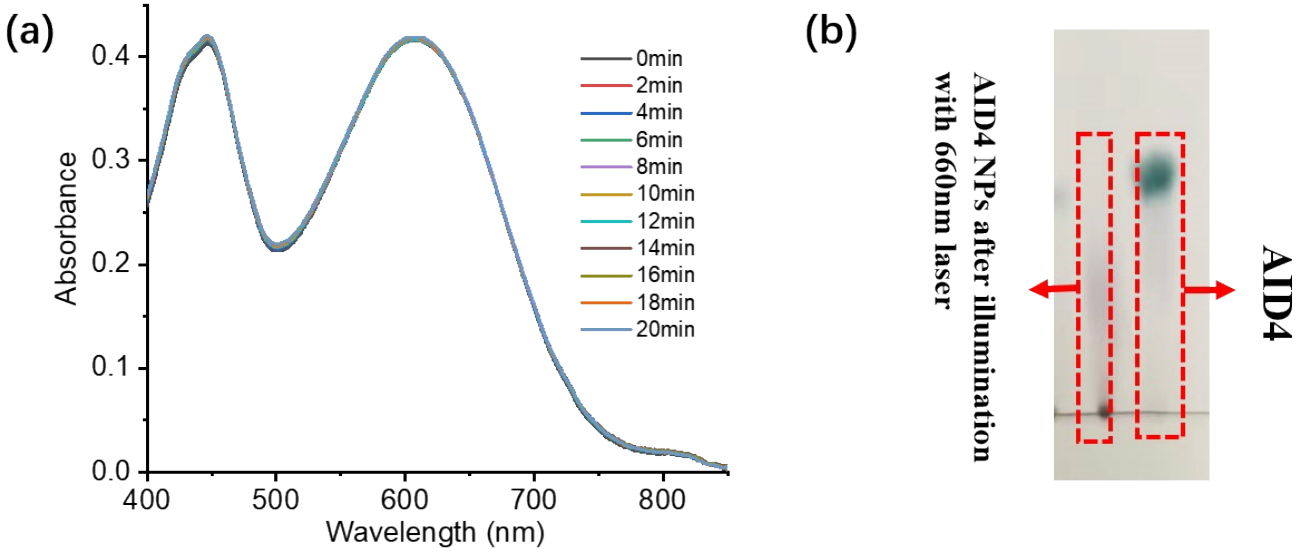

Figure S16. (a) UV absorption spectra of 10 μM AID4 in PMMA after 660 nm laser irradiation (0.4 W/cm^2) with different time. (b) TLC analysis of AID4 and its photolysis products.

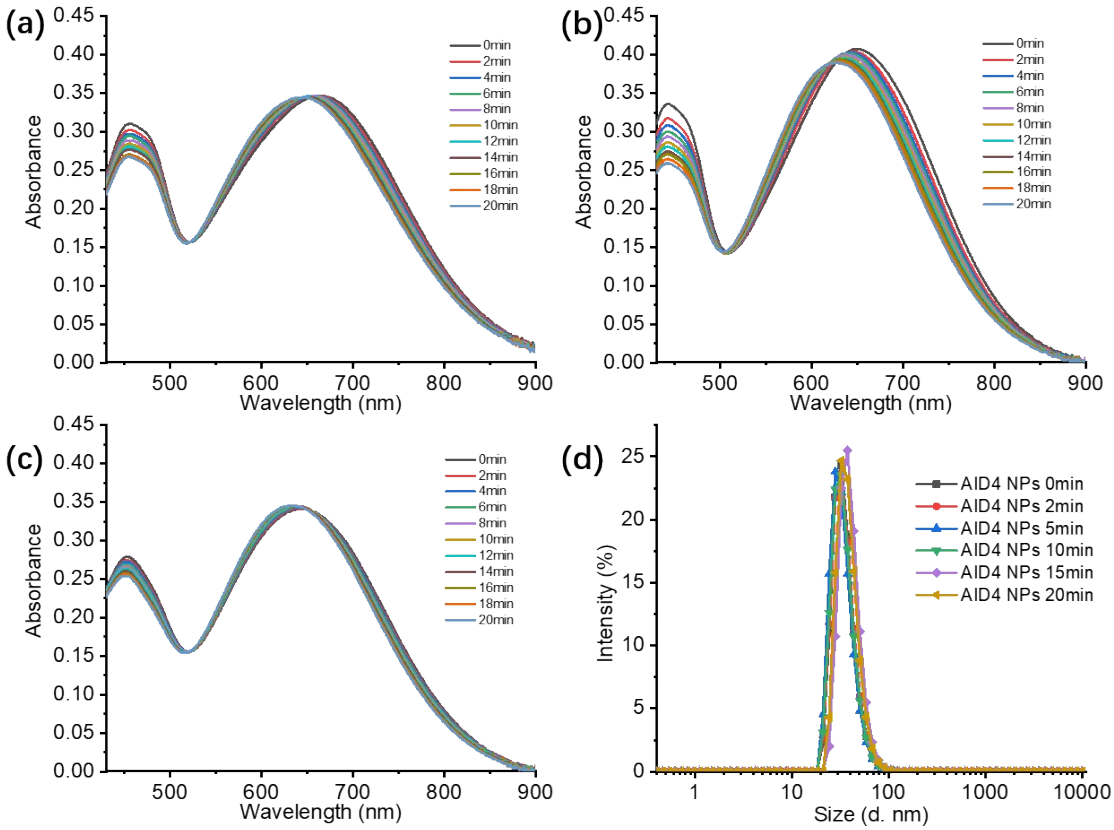

Figure S17. UV-vis absorption spectra of 10 μM (a) AID1 NPs, (b) AID2 NPs and (c) AID3 NPs in water after 660 nm laser irradiation (0.4 W/cm^2) with different time; (d) DLS Size distribution of AID4 NPs after 660 nm laser irradiation with different times measured by DLS in water.

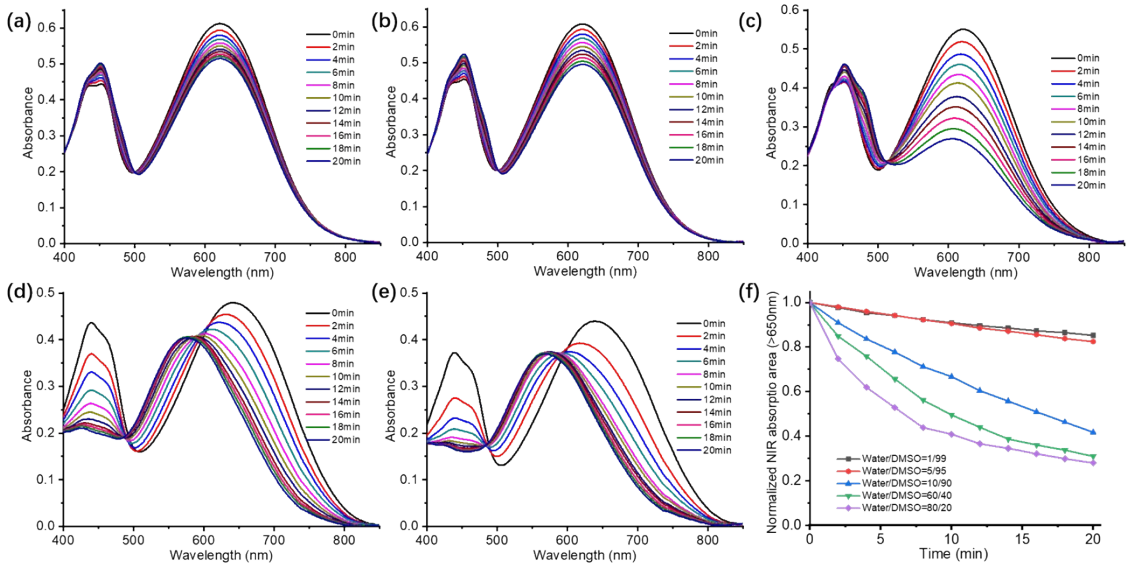

Figure S18. UV absorption spectra of 10 μM AID4 NPs in a mixed solvent of DMSO and water (（a）DMSO/water=99/1;(b) DMSO/water=95/5; （c）DMSO/water=90/10; （d）DMSO/water=40/60; （e）DMSO/water=20/80) after 660 nm laser irradiation (0.4 W/cm^2) with different time; (f) the

absorption area(>650nm) change of AID4 NPs in different ratios of a mixed solvent of DMSO and water with light exposure time.

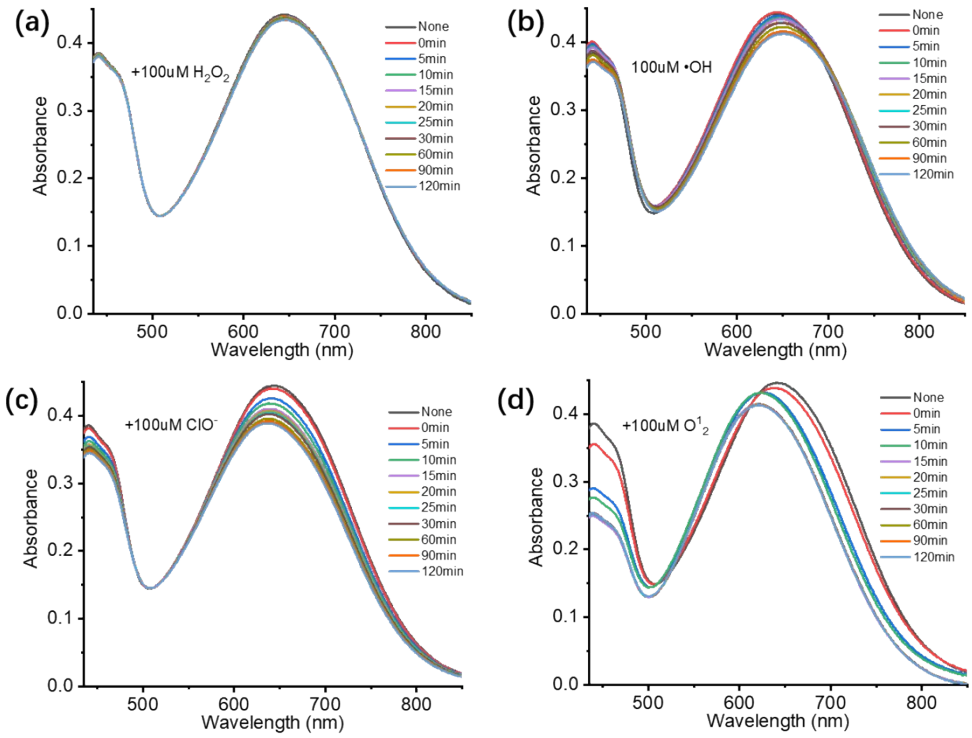

Figure S19. UV-vis absorption spectra of 10μM AID4 in water after adding various oxidizing substances (a) 100μM H_2O_2, (b) 100μM •OH, (c) 100μM ClO^- and (d) 100μM $^1O_2$ (100μM H_2O_2 + 100μM ClO^-) with different reaction time.

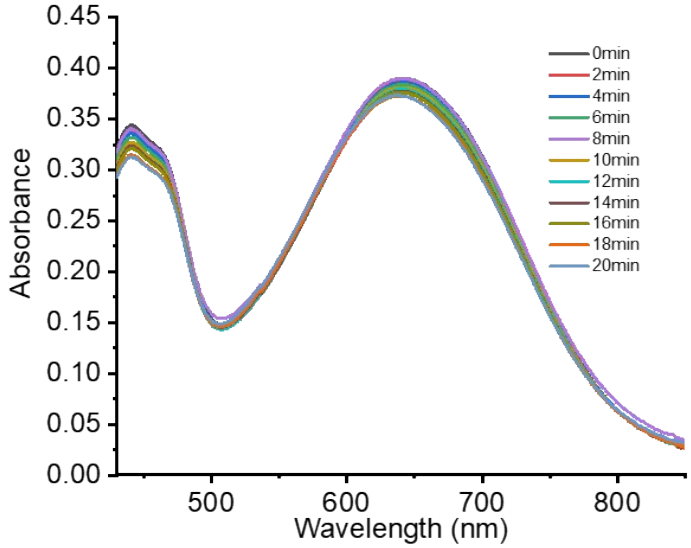

Figure S20. UV-vis absorption spectra of 10 μM AID4 in water under hypoxic environment with increasing irradiation time upon 660 nm laser irradiation (0.4 W cm^{-2}).

,

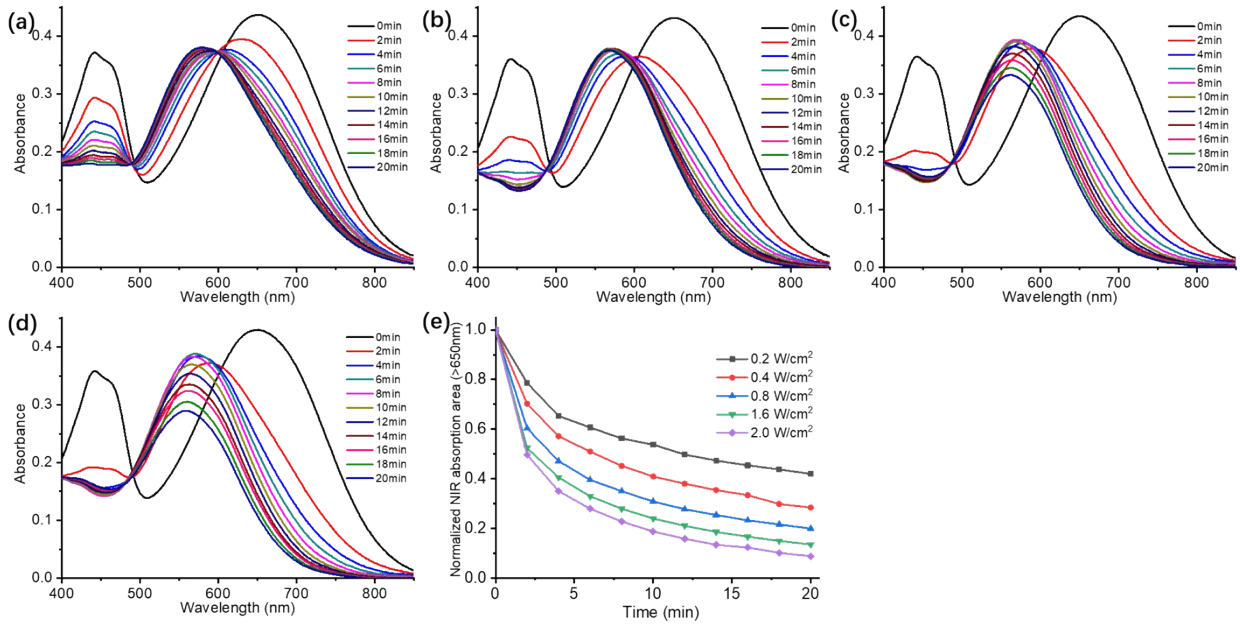

Figure S21. UV absorption spectra of 10 μM AID4 NPs in water after 660 nm laser irradiation with different optical power density (a) 0.2 W/cm^2, (b) 0.8 W/cm^2, (c) 1.6 W/cm^2, (d) 2.0 W/cm^2 for different time; (e) the absorption area(>650nm) change of AID4 NPs after 660 nm laser irradiation with different optical power density for different time.

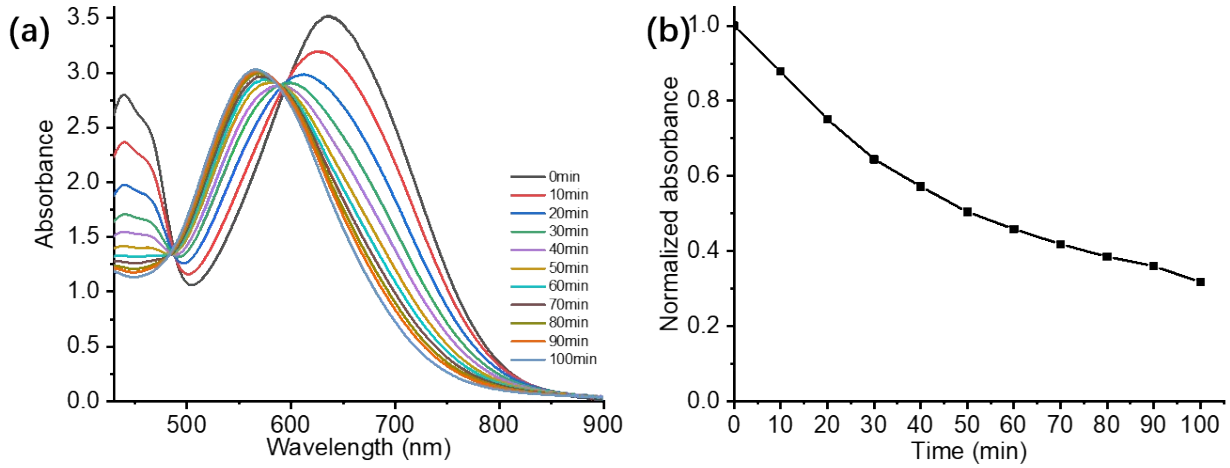

Figure S22. (a) UV absorption spectra of 80 μM AID4 NPs in water after 660 nm laser irradiation (0.4 W/cm^2) with different time; (b) the absorption area(>650nm) change of 80 μM AID4 NPs in water with light exposure time.

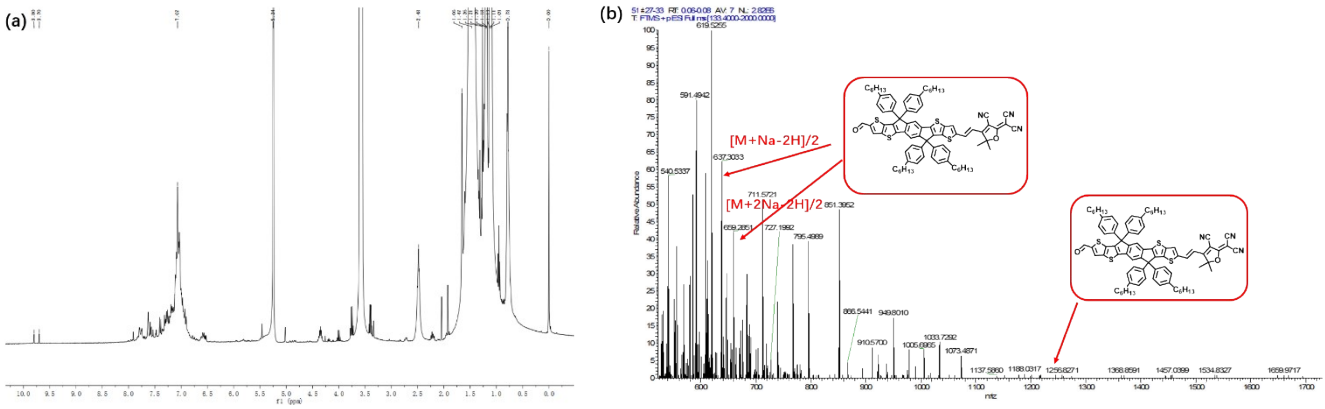

Figure S23. (a) the ^{1}H NMR spectra and (b) the HRMS spectra of photodegradation products of AID4 NPs.

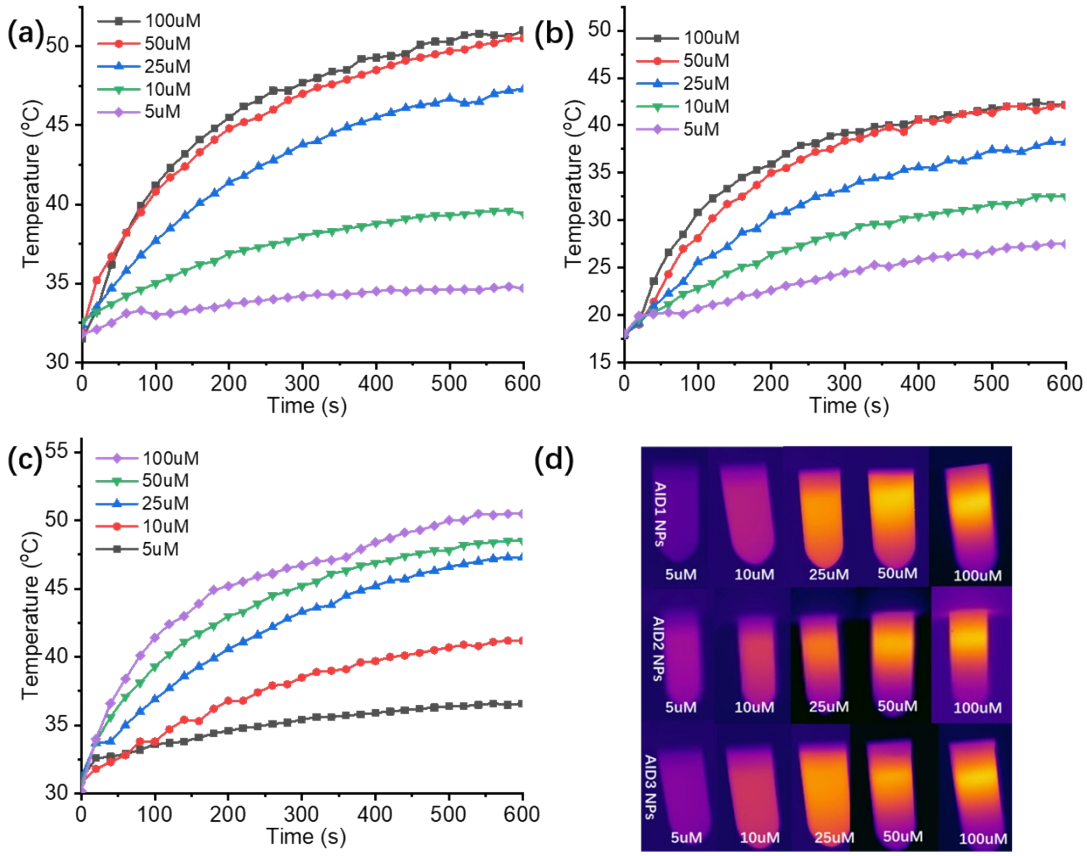

Figure S24. Concentration-dependent temperature variation of (a) AID1 NPs (η =61.9%), (b) AID2 NPs (η =63.3%), (c) AID3 NPs (η =54.7%) solution with 660 nm (0.4 W/cm^2) laser irradiation; IR image of AID 1-3 NPS solution with different concentration after 660 nm laser irradiation (0.4 W cm^{-2}) for 10min.

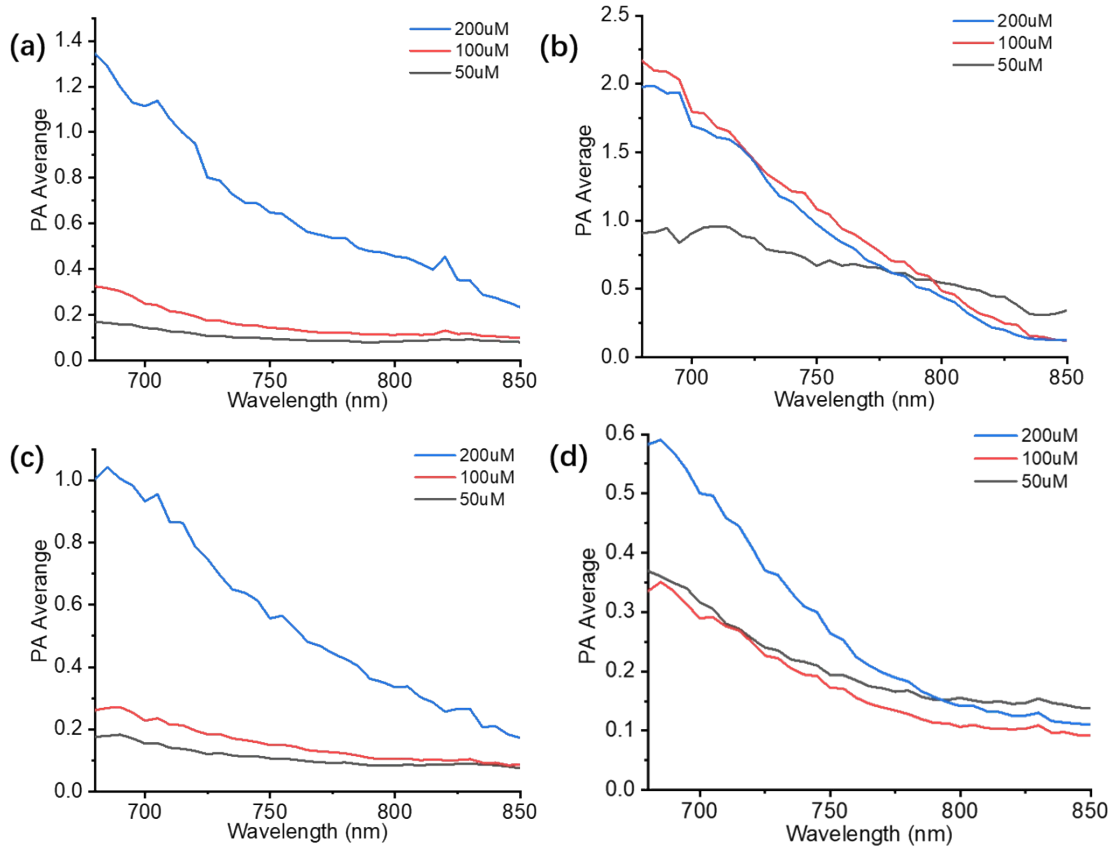

Figure S25. PA spectra of different concentrations of (a) AID1 NPs, (b) AID2 NPs, (c) AID3 NPs and (d) AID4 NPs.

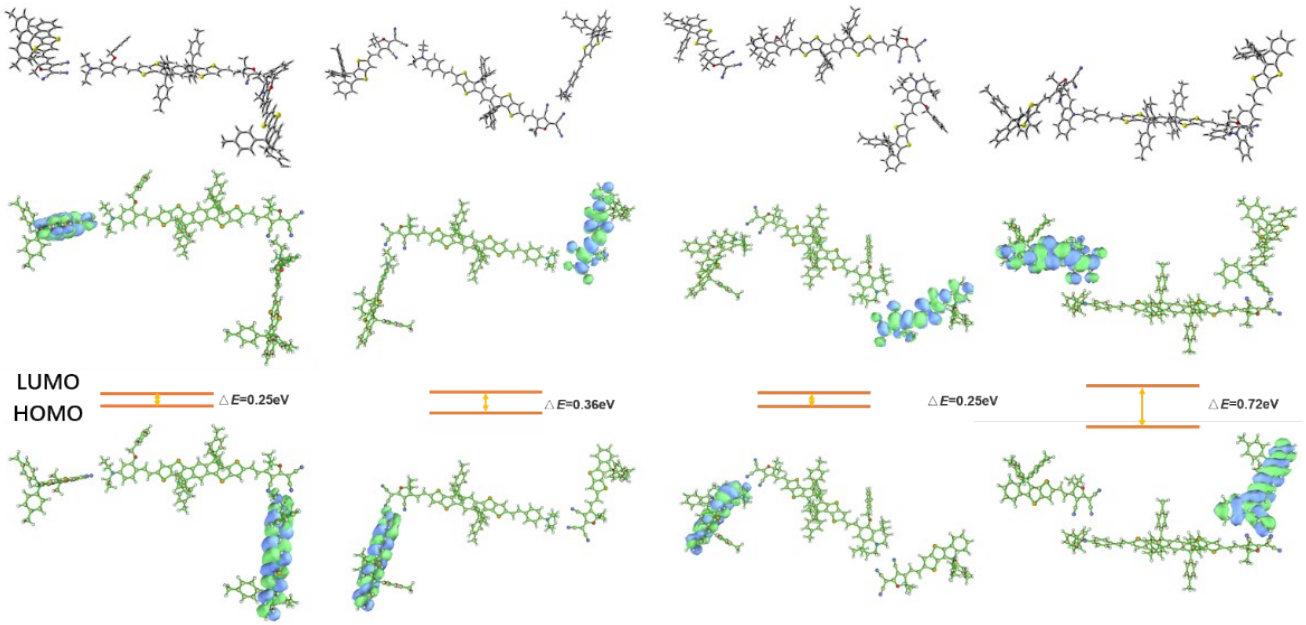

Figure S26. the HOMO–LUMO distribution of AID1-4 in J aggregate state and the energy levels and ΔE values between HOMO and LUMO.

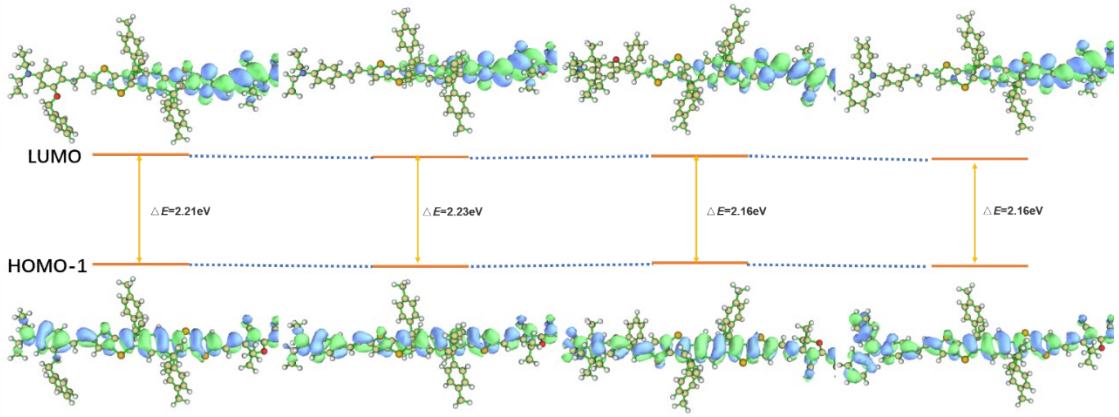

Figure S27. single transition of the maximum contribution for their first excited state near the maximum absorption wavelength when AID 1-4 were in monodisperse state.

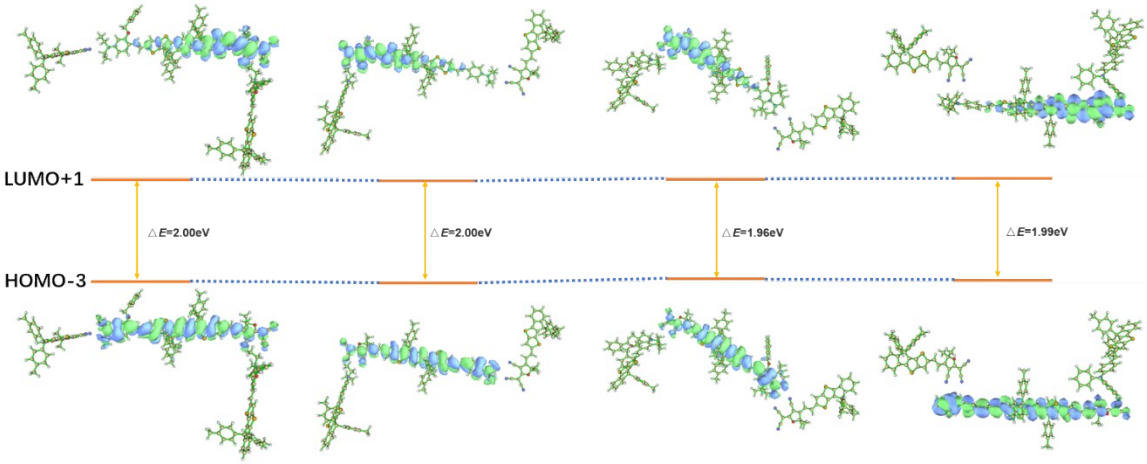

Figure S28. single transition of the maximum contribution for their first excited state near the maximum absorption wavelength when AID 1-4 were in J aggregate state.

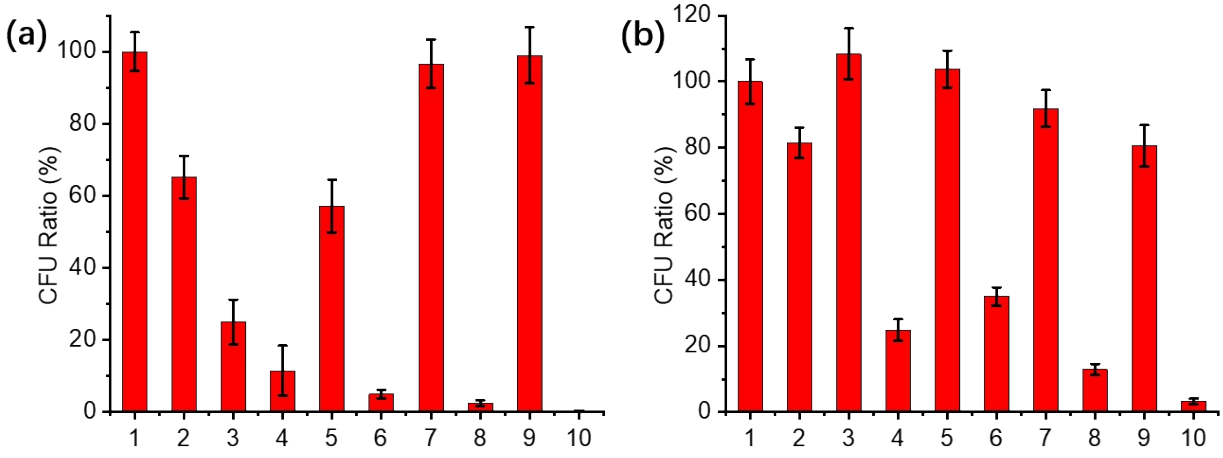

Figure S29. Colony-forming unit (CFU) ratio of (a) *S. Aureus* and (b) *E. coli* after different treatment: (1) None, (2) None with Laser, (3) AID1 NPs in dark, (4) AID1 NPs with laser, (5) AID2 NPs in dark, (6) AID2 NPs with laser, (7) AID3 NPs in dark, (8) AID3 NPs with laser, (9) AID4 NPs in dark, (10) AID4 NPs with laser.

Table S2. (a) the p values of *S. Aureus* in dark; (b) the p values of *S. Aureus* with 660 nm laser irradiation (0.4 W/cm^2, 5 min); (c) the p values of *E. Coli* in dark; (d) the p values of *E. Coli* with 660 nm laser irradiation (0.4 W/cm^2, 5 min).

(a)

	AID4 NPs	AID3 NPs	AID2 NPs	AID1 NPs
None	0.042	0.038	0.045	0.036
AID1 NPs	0.049	0.045	0.049	
AID2 NPs	0.039	0.042		
AID3 NPs	0.041			

(b)

	AID4 NPs	AID3 NPs	AID2 NPs	AID1 NPs
None	0.036	0.046	0.047	0.043
AID1 NPs	0.043	0.038	0.037	
AID2 NPs	0.042	0.046		
AID3 NPs	0.035			

(c)

	AID4 NPs	AID3 NPs	AID2 NPs	AID1 NPs
None	0.045	0.042	0.041	0.029
AID1 NPs	0.046	0.043	0.039	
AID2 NPs	0.049	0.038		
AID3 NPs	0.048			

(d)

	AID4 NPs	AID3 NPs	AID2 NPs	AID1 NPs
None	0.043	0.046	0.042	0.048
AID1 NPs	0.038	0.041	0.036	
AID2 NPs	0.047	0.038		
AID3 NPs	0.038			

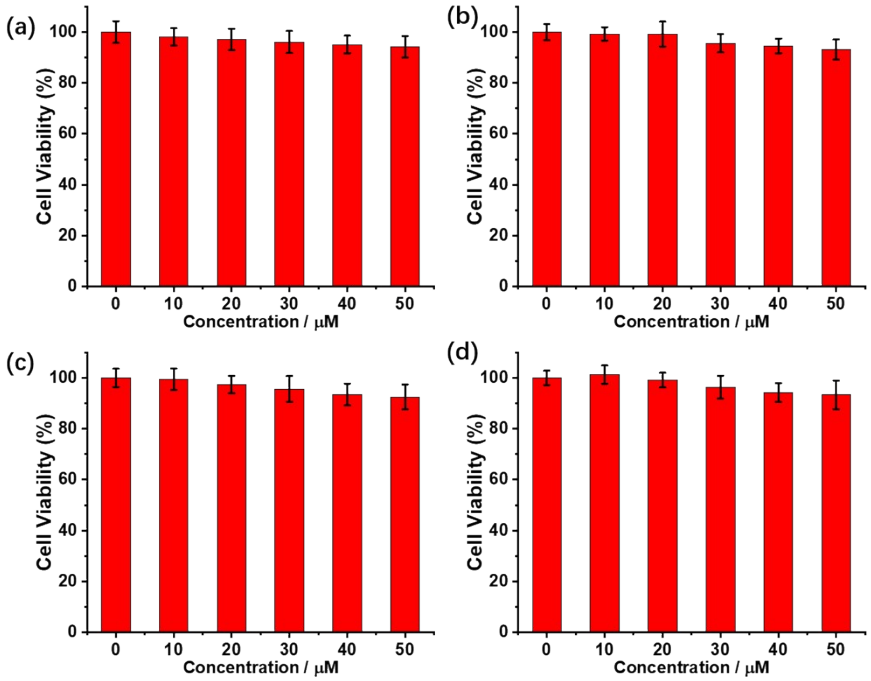

Figure S30. Cell viability of 4T1 cells at varied concentrations of (a) AID1 NPs, (b) AID2 NPs, (c) AID3 NPs and (d) AID4 NPs in dark using CCK8 assay.

Table S3. The p values of Cell viability of 4T1 cells at varied concentrations of (a) AID1 NPs, (b) AID2 NPs, (c) AID3 NPs and (d) AID4 NPs

(a)

	0	10	20	30	40
50	0.048	0.058	0.043	0.054	0.037
40	0.052	0.047	0.052	0.032	
30	0.039	0.042	0.044		
20	0.042	0.039			
10	0.032				

(b)

	0	10	20	30	40
50	0.041	0.038	0.036	0.034	0.047
40	0.047	0.046	0.042	0.042	
30	0.049	0.042	0.054		
20	0.024	0.029			
10	0.038				

(c)

	0	10	20	30	40
50	0.050	0.038	0.047	0.036	0.046
40	0.041	0.045	0.043	0.042	
30	0.041	0.042	0.047		
20	0.046	0.032			
10	0.038				

(d)

	0	10	20	30	40
50	0.041	0.048	0.054	0.045	0.039
40	0.056	0.057	0.032	0.026	
30	0.049	0.032	0.044		
20	0.032	0.049			
10	0.042				

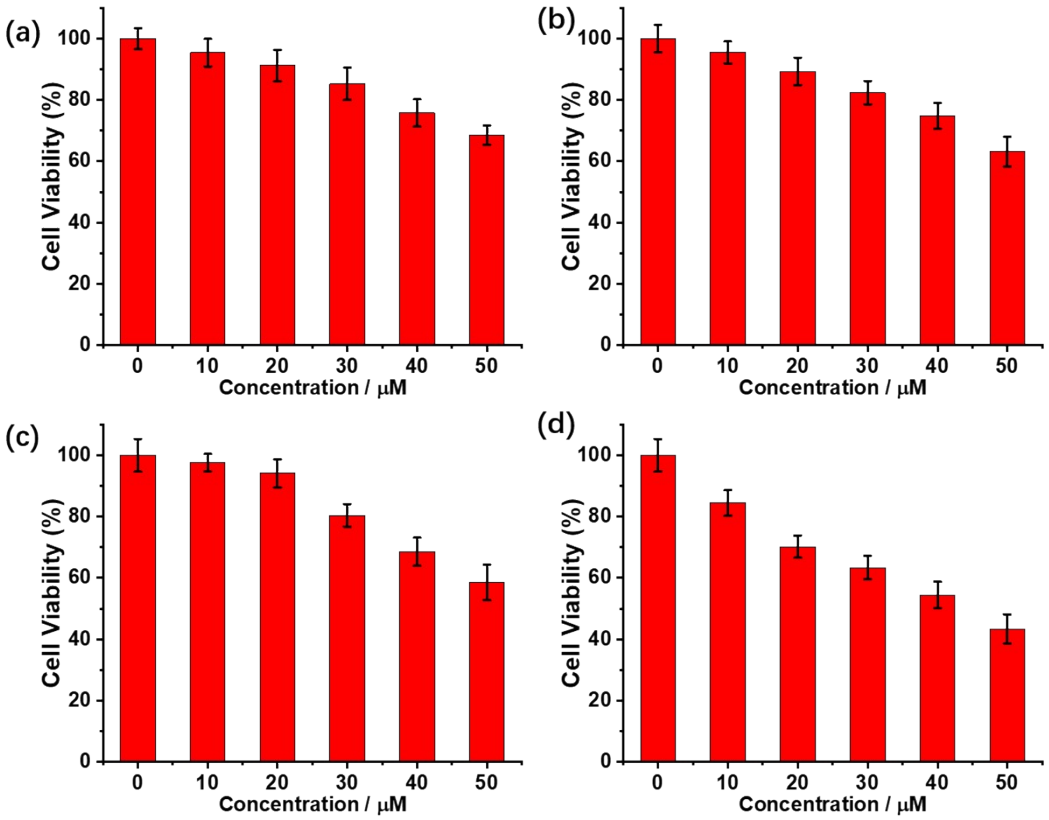

Figure S31. Cell viability of 4T1 cells at varied concentrations of (a) AID1 NPs, (b) AID2 NPs, (c) AID3 NPs and (d) AID4 NPs exposed to 660nm laser (0.4W/cm^2) for 10 minutes using CCK8 assay.

Table S4. The p values of Cell viability of 4T1 cells at varied concentrations of (a) AID1 NPs, (b) AID2 NPs, (c) AID3 NPs and (d) AID4 NPs exposed to 660nm laser (0.4W/cm^2) for 10 minutes using CCK8 assay.

(a)

	0	10	20	30	40
50	0.039	0.047	0.036	0.056	0.054
40	0.041	0.056	0.047	0.053	
30	0.050	0.053	0.053		
20	0.053	0.028			
10	0.043				

(b)

	0	10	20	30	40
50	0.036	0.045	0.055	0.042	0.049
40	0.040	0.035	0.040	0.045	
30	0.051	0.031	0.041		
20	0.043	0.043			
10	0.021				

(c)

	0	10	20	30	40
50	0.051	0.043	0.032	0.041	0.050
40	0.039	0.035	0.039	0.045	
30	0.052	0.032	0.056		
20	0.055	0.051			
10	0.045				

(d)

	0	10	20	30	40
50	0.037	0.044	0.029	0.043	0.057
40	0.031	0.026	0.031	0.053	
30	0.052	0.021	0.023		
20	0.021	0.018			
10	0.043				

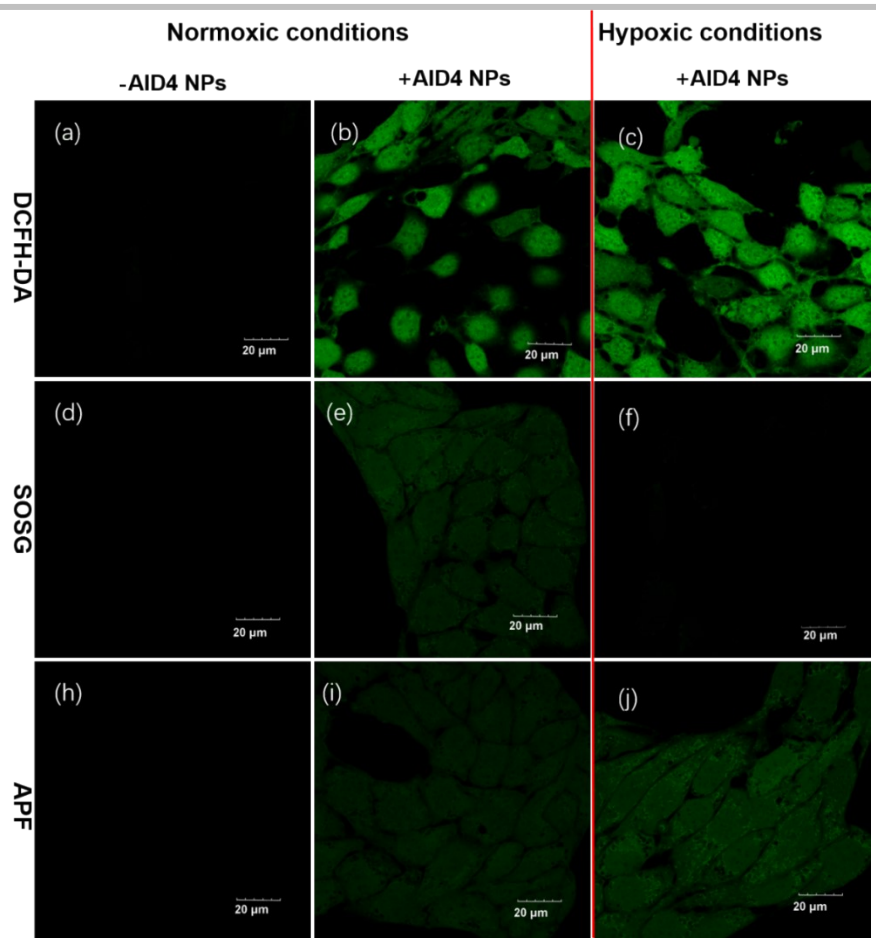

Figure S32. ROS detection in 4T1 cells under normoxia and hypoxia conditions using (a-c) DCFH-DA, (d-f) SOSG and (h-j) AFP as total ROS, $^1O_2$ and •OH fluorescence indicator.

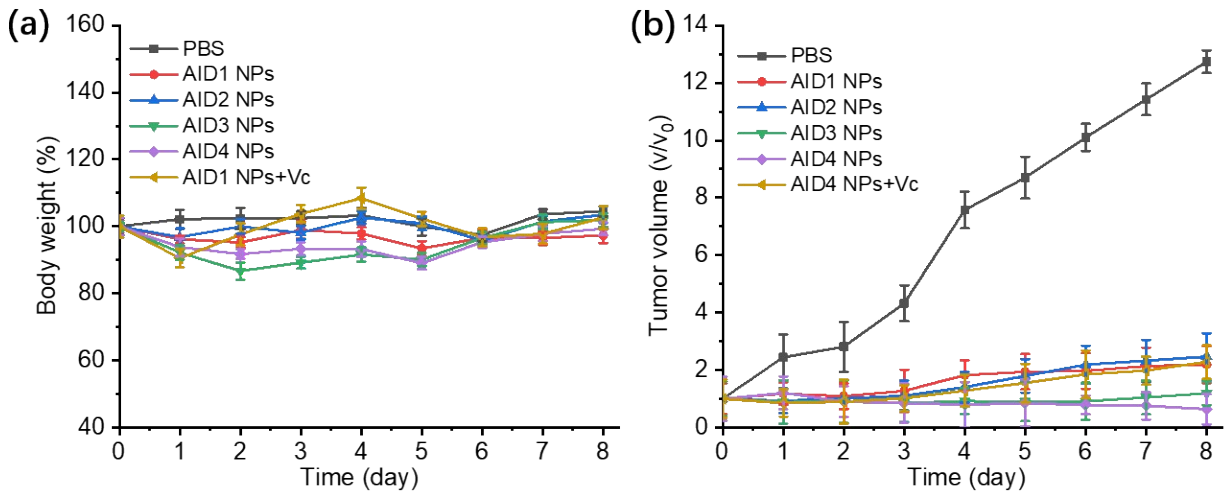

Figure S33. (a) relative body weight changes of mice during different treatments. (b) curve of the tumor size with the time.

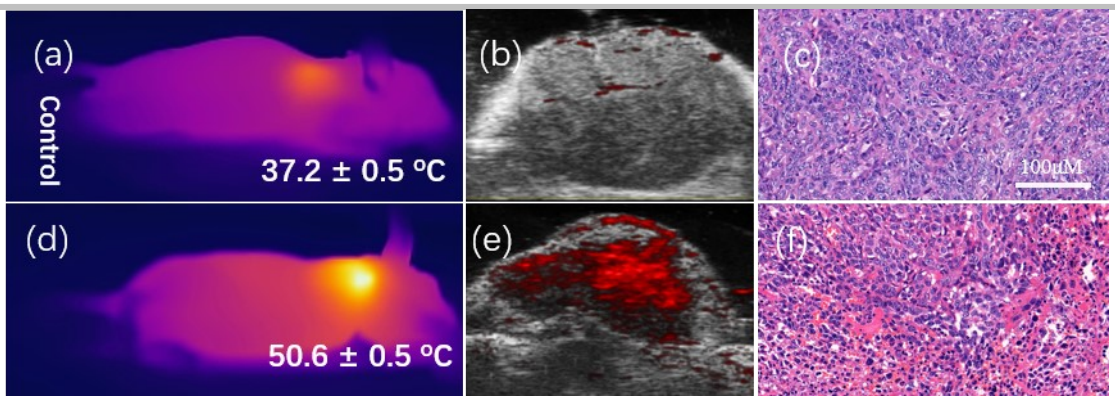

Figure S34. IR thermal imaging of 4T1 tumor-xenograft mice irradiated by 660 nm laser (0.4 W/cm^2) for 10 min after in vivo injection of (a) PBS and (d) Vitamin C + AID4 NPs ; (b) and (e) corresponding PAI; (c) and (f) tumor H&E-stained slices of the mice after the phototherapy.

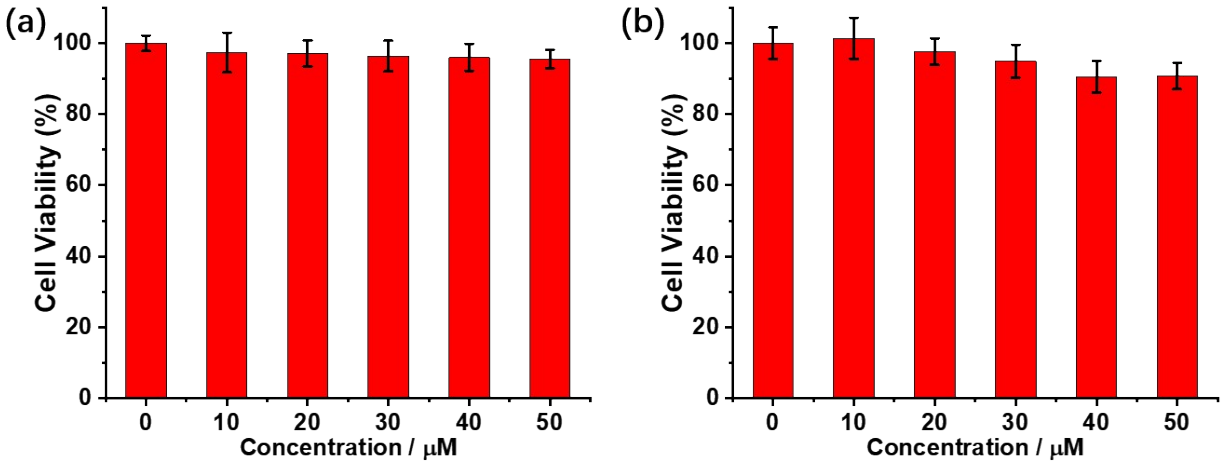

Figure S35. Cell viability of 4T1 at varied concentrations of photodegradation products of AID4 NPs with different concentrations using CCK8 assay (a) in dark and (b) exposed to 660nm laser (0.4W/cm^2) for 10 minutes.

Table S5. The p values of cell viability of 4T1 at varied concentrations of photodegradation products of AID4 NPs with different concentrations using CCK8 assay (a) in dark and (b) exposed to 660nm laser (0.4W/cm^2) for 10 minutes.

(a)

	0	10	20	30	40
50	0.043	0.037	0.020	0.031	0.014
40	0.039	0.052	0.038	0.043	
30	0.043	0.038	0.047		
20	0.035	0.029			
10	0.034				

(b)

	0	10	20	30	40
50	0.052	0.034	0.038	0.035	0.028
40	0.047	0.042	0.034	0.039	
30	0.025	0.036	0.027		
20	0.028	0.045			
10	0.023				

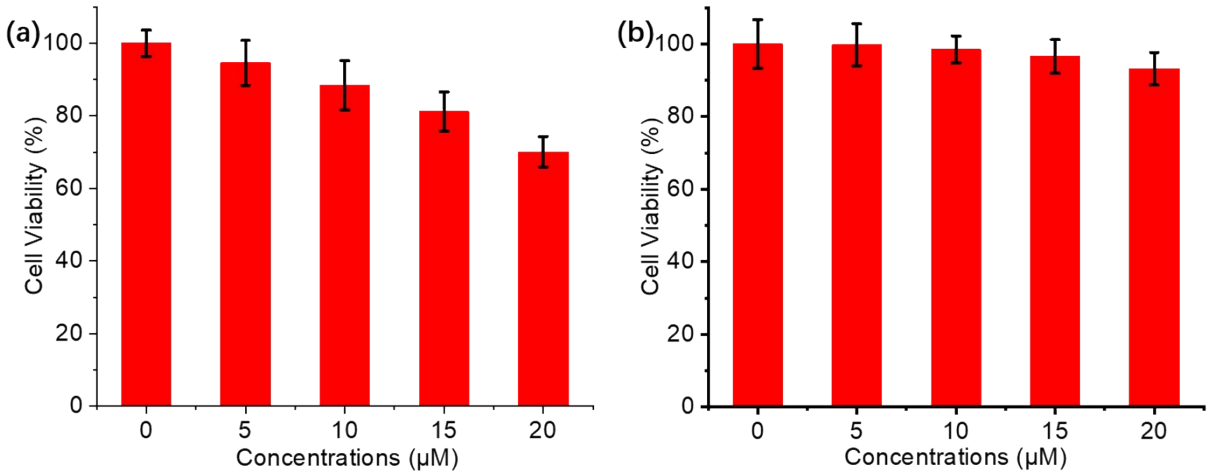

Figure S36. (a) Cell viability of L929 cells at varied concentrations of (a) Methylene blue after laser irradiation for 30min, (b) AID4 NPs after laser irradiation for 30min.

Table S6. The p values of cell viability of L929 cells at varied concentrations of (a) Methylene blue after laser irradiation for 30min, (b) AID4 NPs after laser irradiation for 30min.

(a)

	0	5	10	15
20	0.038	0.030	0.036	0.045
15	0.045	0.036	0.042	0.023
10	0.046	0.053		
5	0.024			

(b)

	0	5	10	15
20	0.042	0.053	0.028	0.039
15	0.053	0.045	0.035	0.037
10	0.034	0.041		
5	0.035			

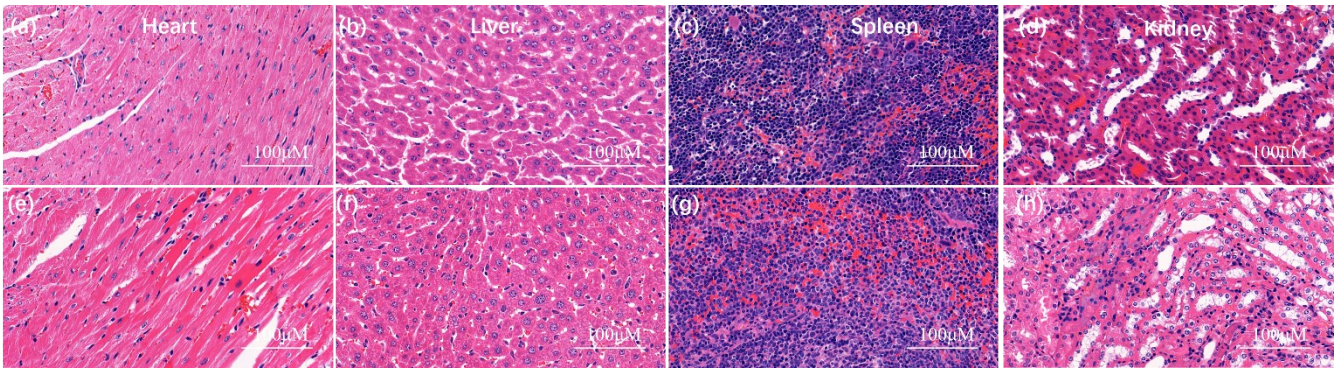

Figure S37. the H&E-stained slices of the (a) heart, (b) liver, (c) spleen and (d) kidney of healthy mice; the H&E-stained slices of the (e) heart, (f) liver, (g) spleen and (h) kidney after therapy using AID4 NPs.

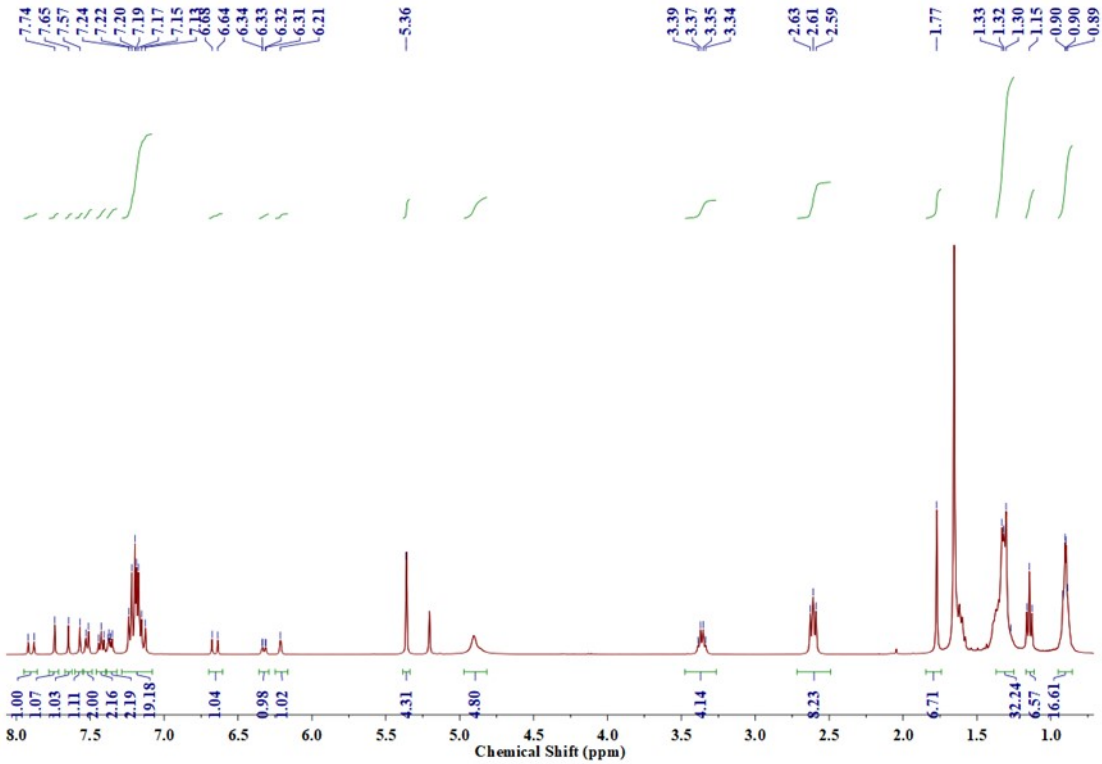

Figure S38. the ^{1}H NMR spectra of AID1

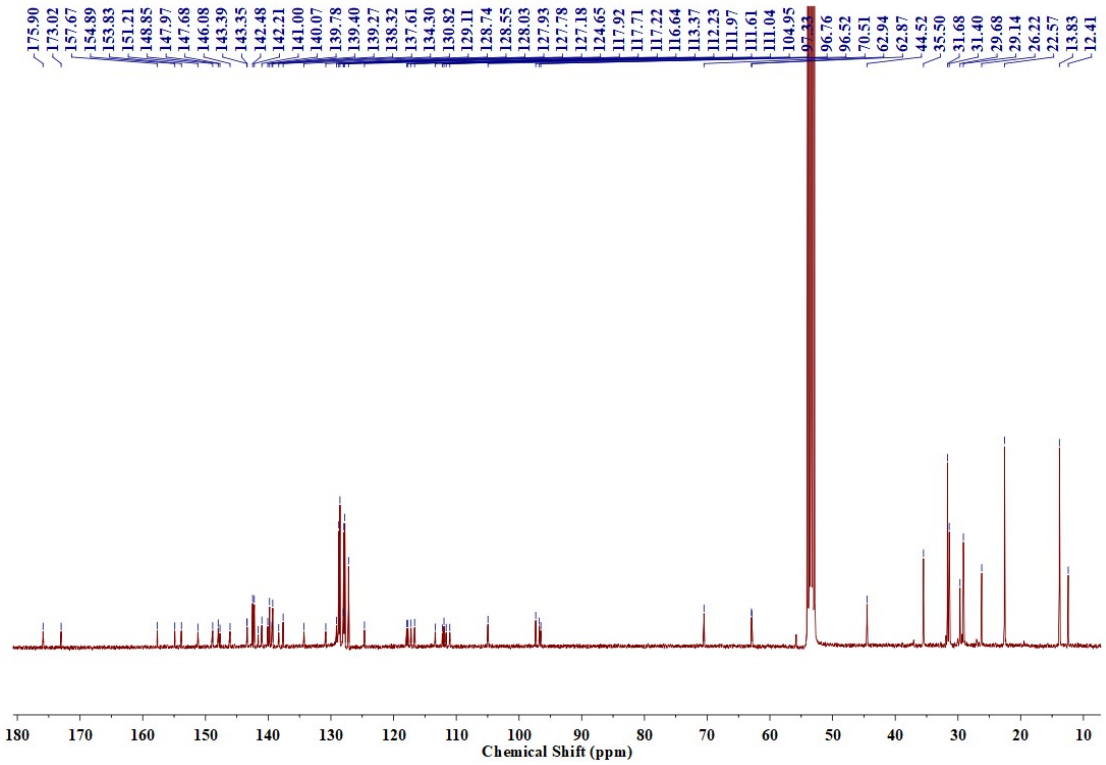

Figure S39. the ^{13}C NMRspectra of AID1

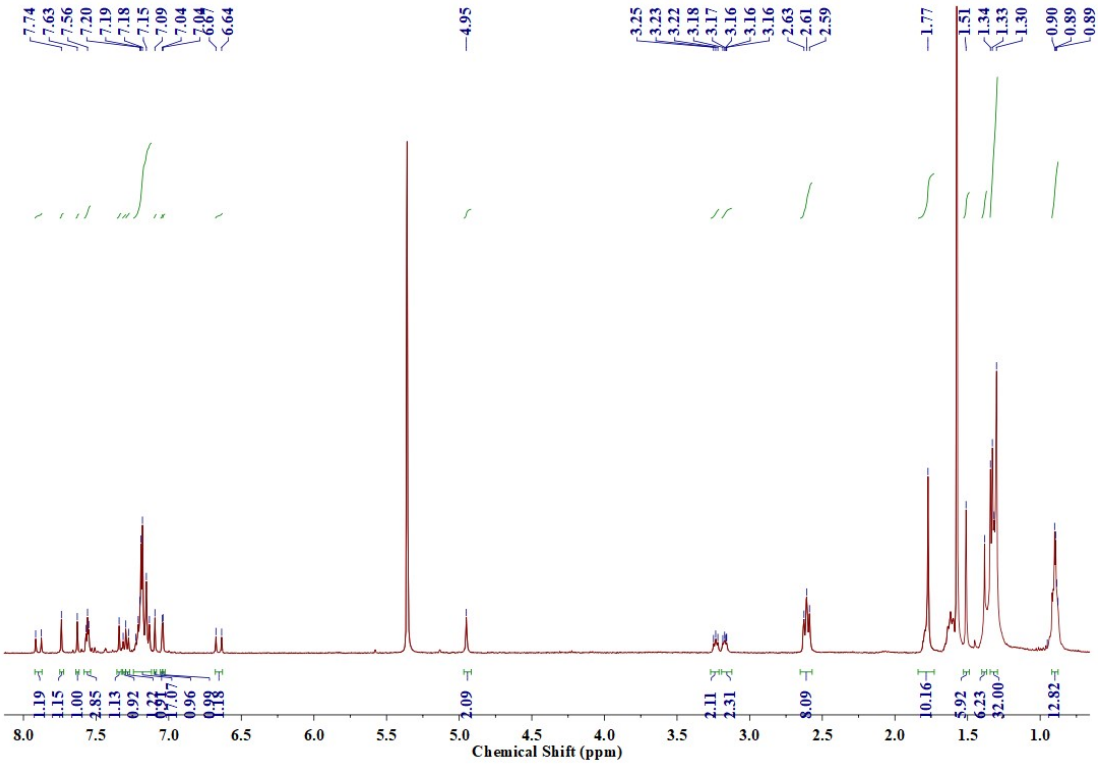

Figure S40. the ^{1}H NMR spectra of AID2

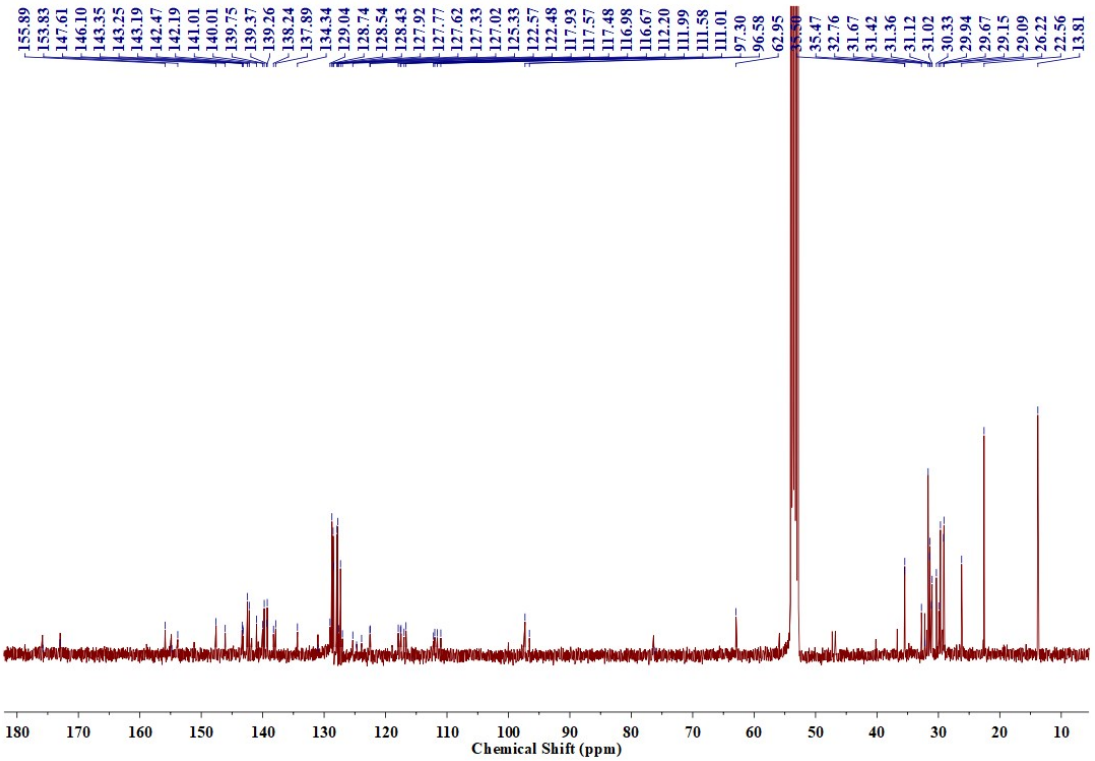

Figure S41. the ^{13}C NMR spectra of AID2

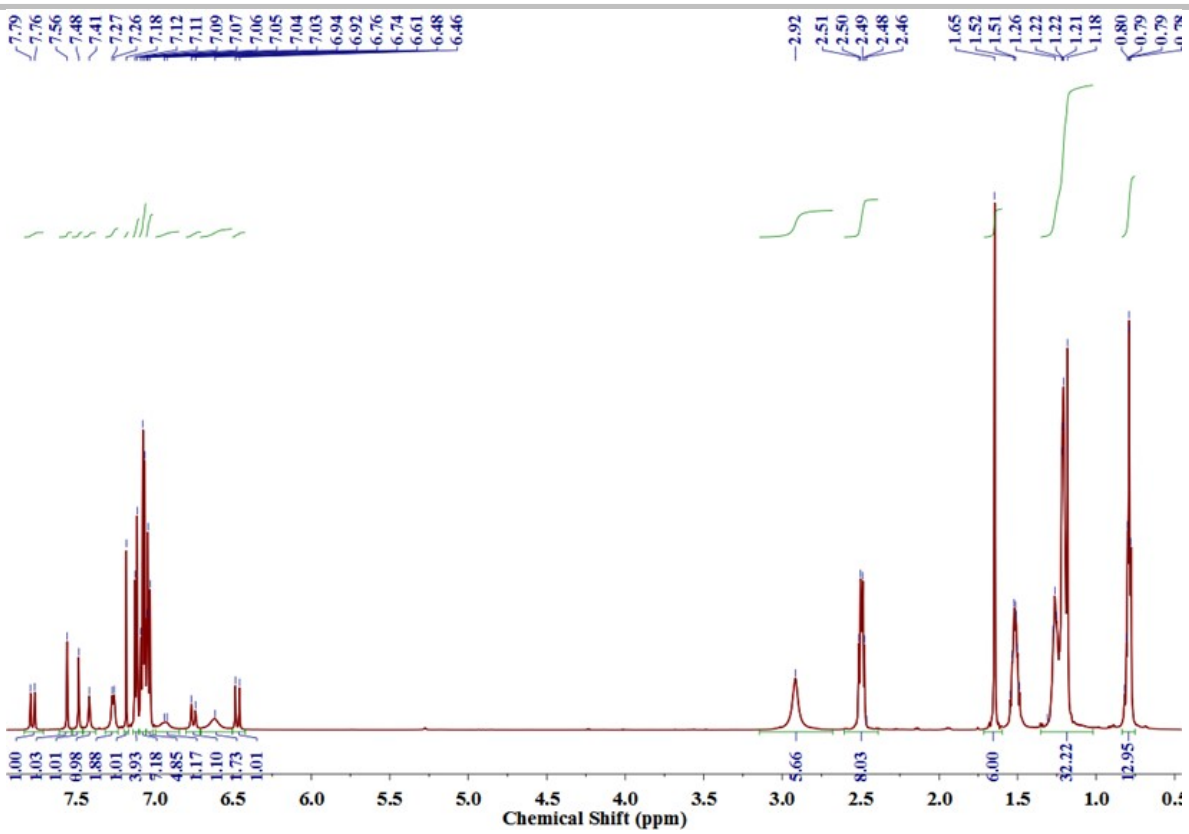

Figure S42. the ^{1}H NMR spectra of AID3

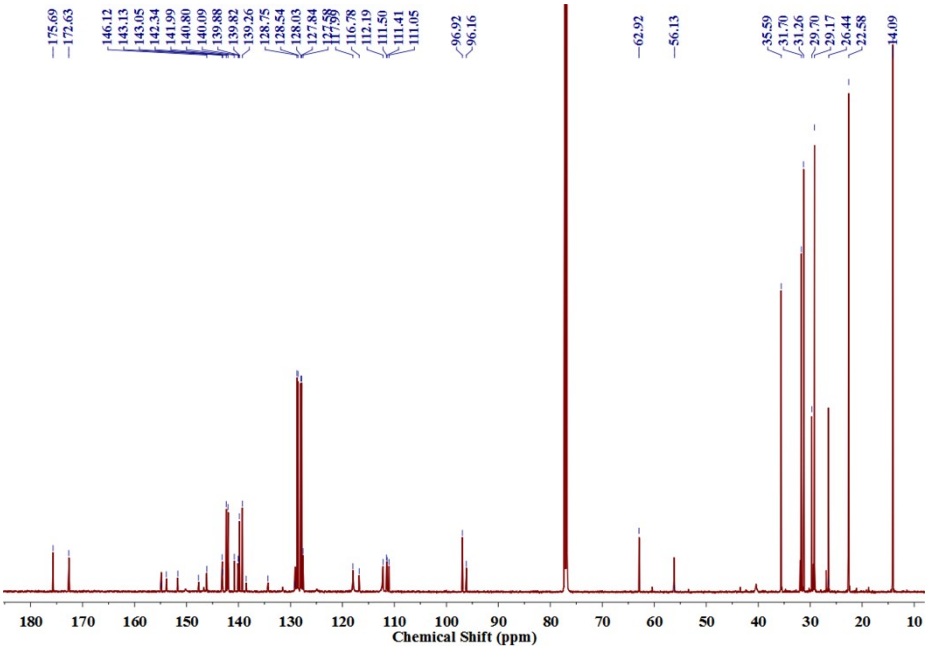

Figure S43. the ^{13}C NMR spectra of AID3

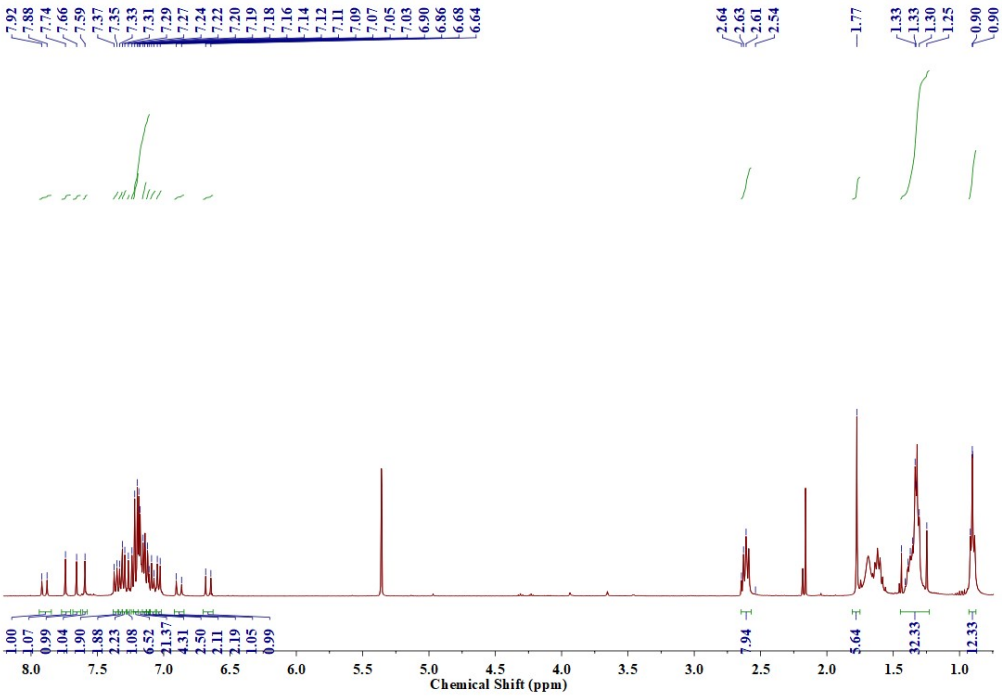

Figure S44. the ^{1}H NMR spectra of AID4

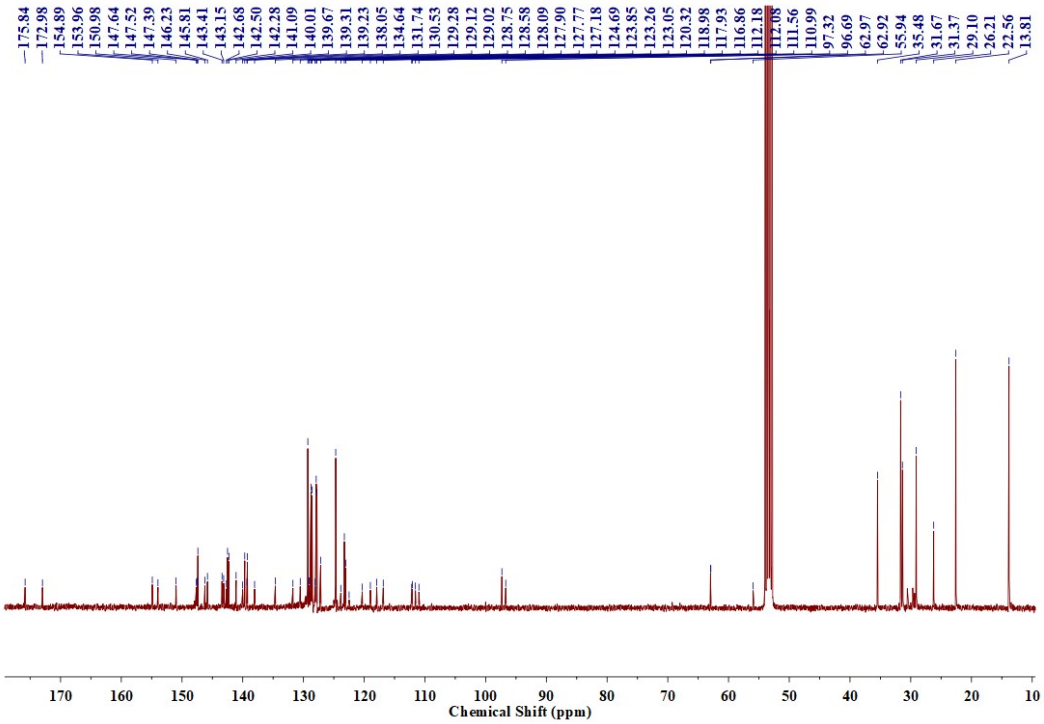

Figure S45. the ^{13}C NMR spectra of AID4

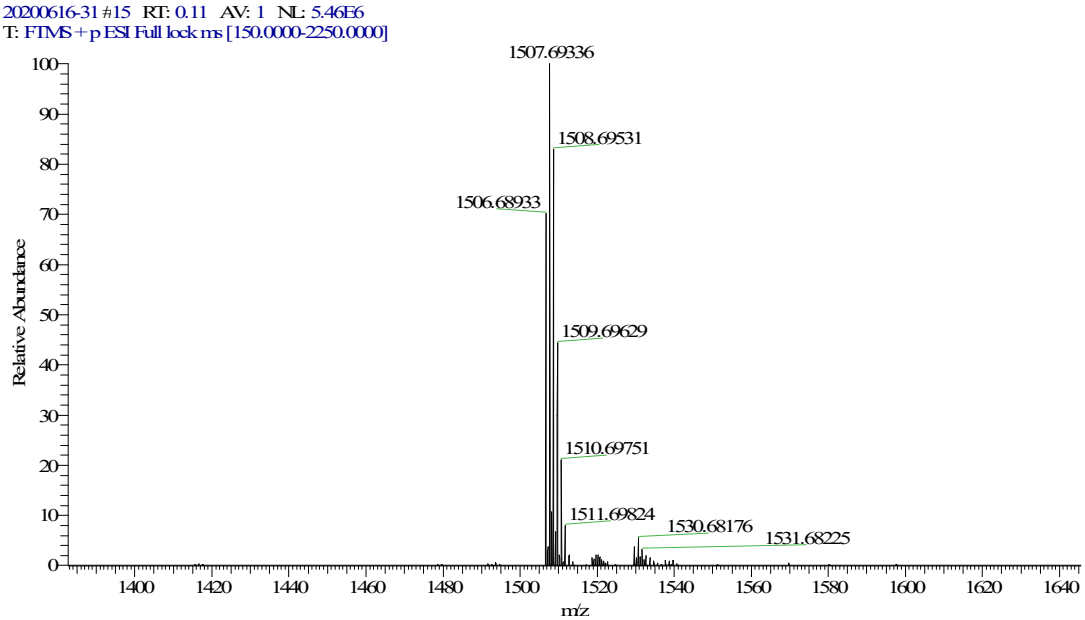

Figure S46. The HRMS spectra of AID1

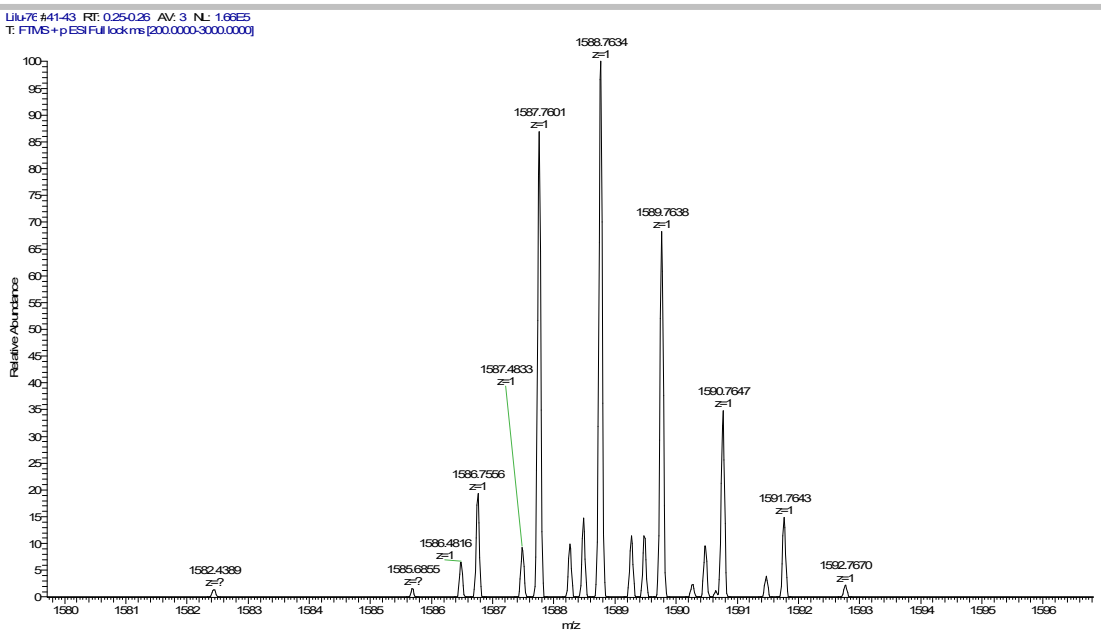

Figure S47. The HRMS spectra of AID2

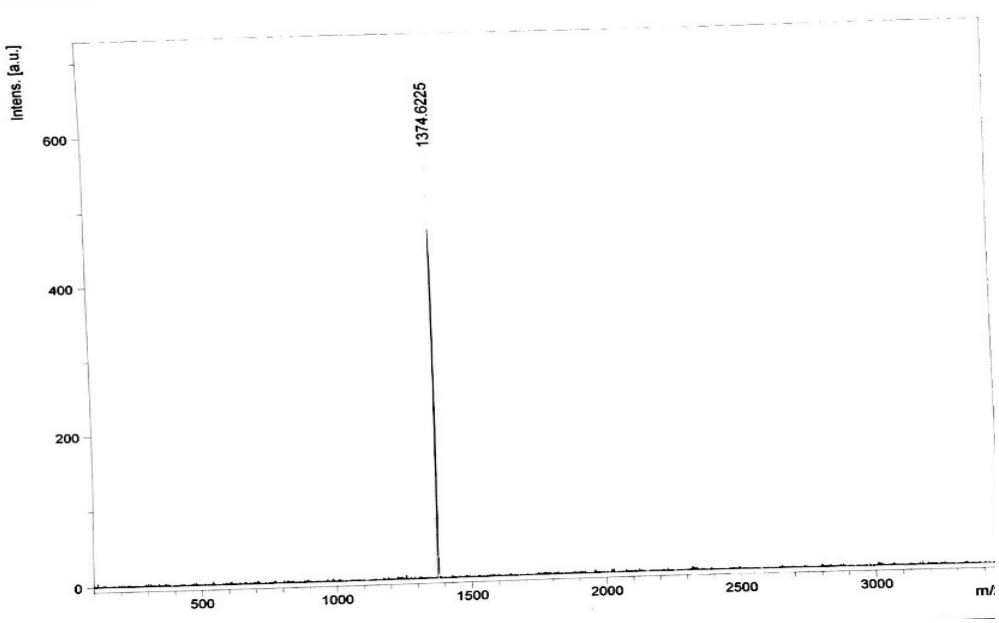

Figure S48. The HRMS spectra of AID3

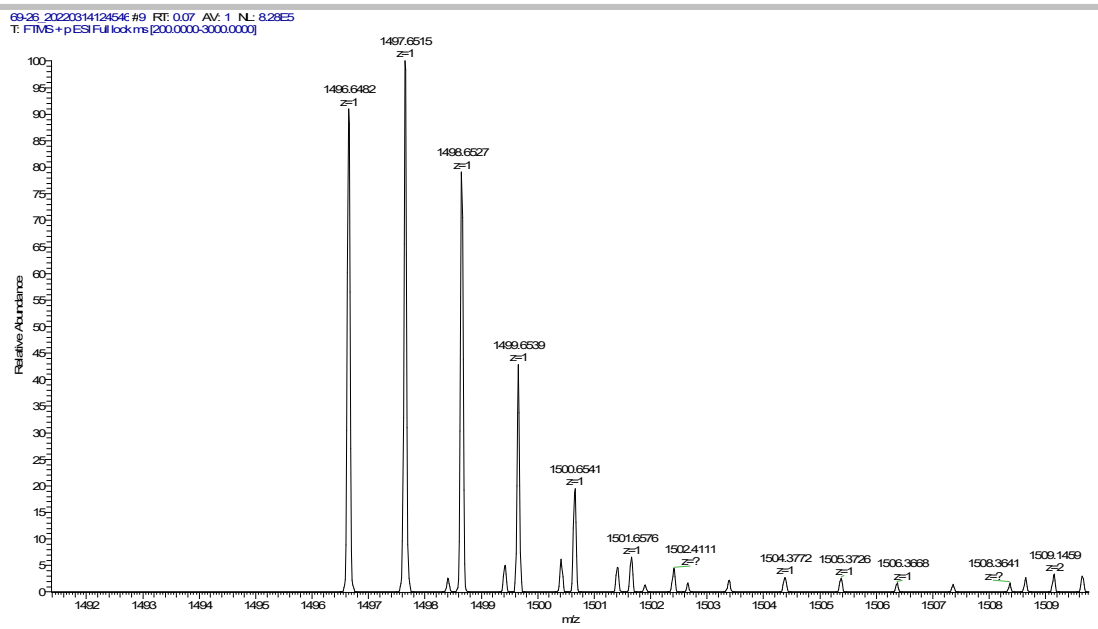

Figure S49. The HRMS spectra of AID4

References

[1] Lu T, Chen F. Multiwfn: a multifunctional wavefunction analyzer. Journal of computational chemistry, 2012, 33(5): 580-592.